OTC-27695-MS

Heavy Lift Dynamics, Sewol Ferry Offshore Salvage

W.P. Stewart, P. George, and W. Ashley, Stewart Technology Associates, A. Guha, ABS, V. Achanta, Ace Engineers

This paper was prepared for presentation at the Offshore Technology Conference held in Houston, Texas, USA, 1–4 May 2017.

Abstract

The Sewol Ferry sank off Korea in 2014 with the loss of 304 lives. The remains of 9 victims remain within wreck and cannot be reached by divers. This paper describes some of the heavy lift engineering involved in the salvage of the 146-meter long ferry, in one piece, from a depth of 44 meters in the ocean, resting on its port side.

A method for calculating the interaction of the vessel stern with the seabed (ground reaction) is described as the bow of the 8,000-ton vessel is raised to place lifting beams to be used in the side lift.

Significant difficulties, associated with geotechnical issues, resulting in project delays are described.

Calculation methods are presented for determining the large trapped water mass and the large frequency and depth dependent added mass of the submerged vessel (greater than 120,000 tons). Coupled dynamic time domain simulations of the initial bow lift, followed by the side lift onto a floating vessel are presented. A total of 34 HMPE synthetic slings are used to attach a 1,200-ton purpose-built lifting frame to the ZPMC 12,000-ton revolving crane.

Wave forecast data from three sources are compared with continuously measured data from a directional wave buoy at the site. The difficulties in predicting and controlling the heel of the vessel with a combination of added buoyancy, slings and geotechnical forces are described for the failed attempt at the first bow lift and for the final bow lift. Dynamic sling tensions are shown calculated for the upper HMPE slings and the lower steel rope vertical and balance slings from the lifting frame to the lifting beams. Detailed static and quasi-dynamic FEA results are described for the Sewol hull, together with buckling checks.

MV Sewol Characteristics

- Length 145.6m
- Beam 22m
- Lightship 6213t
- Displacement 7742t (at time of sinking)

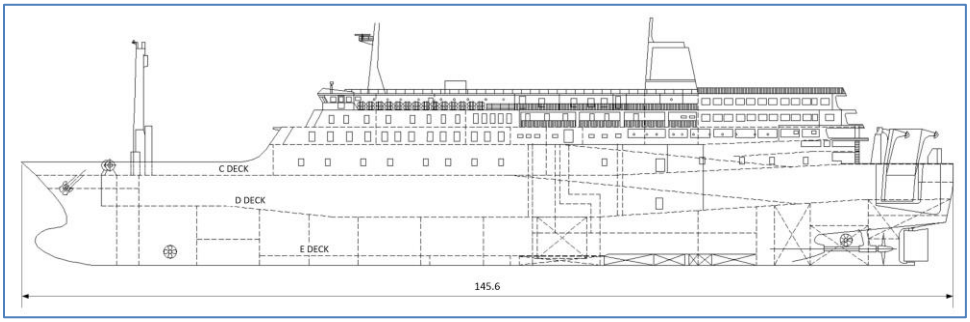

Figure 1 - Profile View of the SEWOL ferry

MV Sewol Accident

The MV Sewol was a RoPax vessel built in 1994. She sank off southwest Korea on April 16, 2014 with the loss of 304 lives, many of them school children. The captain was found guilty of murder. The vessel capsized and sank in 44m water depth, coming to rest on its port side on a level seabed.

Figure 2 – Sewol Listing and Sinking

Figure 3 – Sewol Upturned and 98% Below Water

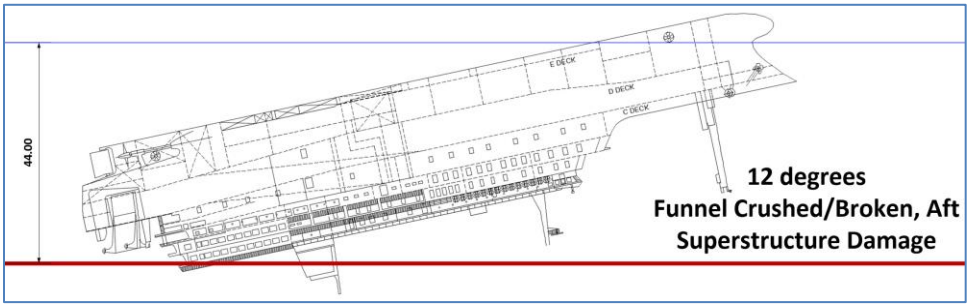

Figure 4 - Profile View of the Upturned SEWOL Before Finally Sinking Completely

In the final stages of sinking, the vessel rolled onto her port side. Inspections revealed the hull was largely intact with some crushing damage to the port aft superstructure and a severely damaged funnel.

Recovery of Bodies

Divers searched for missing bodies until November, 2015. The last body found was in October. Nine bodies were still missing at the time of writing this paper. They are believed to be inside the wreck, probably in the damaged superstructure area.

Salvage Plan

The salvage plan was agreed in July 2016 and work commenced in August. The hull was to be raised in one piece and taken to shore. The salvage was planned in four stages.

- Stage 1 – Add buoyancy and lift bow underwater. Place lifting beams beneath hull and lower vessel onto the beams.
- Stage 2 – Modify buoyancy arrangement and raise hull partially out of water using a large crane and a lifting frame.
- Stage 3 – Place hull onto a submerged floating drydock and refloat drydock, bringing Sewol above water, and tow to shore.
- Stage 4 – Offload Sewol from drydock to shore using SPMT (self-propelled modular transporter).

Figures illustrating the key stages in the salvage plan are shown below. Initially the hull was lying horizontally on the seabed with no more than 1 meter of penetration observed.

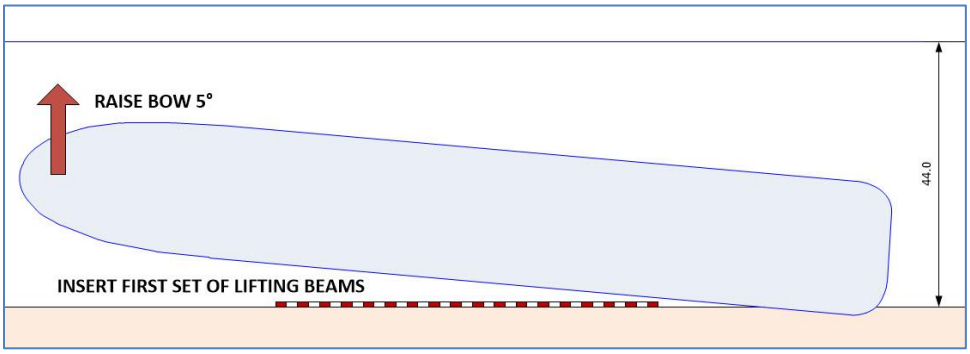

Figure 5 – Salvage Stage 1A, Raise Bow 5° and Insert First Set of Lifting Beams

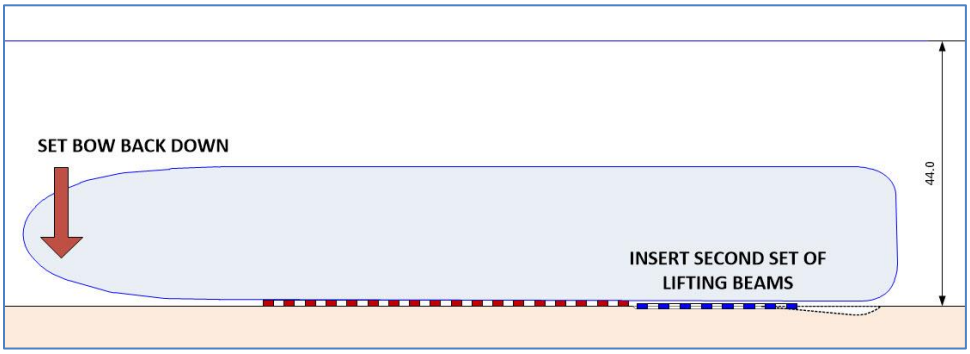

Figure 6 – Salvage Stage 1B, Set Bow Back Down and Insert Second Set of Lifting Beams

Note that the stern is shown pushing into the seabed in Figure 5, as the bow is raised. Then in Figure 6 the hull is shown sitting horizontal and slightly raised on the first set of lifting beams and a small amount of excavation is planned to enable the insertion of the second set of lifting beams.

At each stage of the salvage a large amount of additional buoyancy is used. Some buoyancy is achieved by filling internal tanks with air. Some buoyancy is achieved with airbags deployed inside the hull. Some buoyancy is achieved with external pontoons. Details are provided later in this paper.

After the final 8 lifting beams have been positioned beneath the hull, the plan called for the main lifting frame to be positioned on a cargo barge above the hull, with the balance slings attached. Then the vertical steel wire rope slings would be connected to the 26 lifting beams (with 8 additional wire slings around the hull without lifting beams).

The 12,000t heavy lift vessel, the Zhen Hua 30, was planned for the project, but this changed during the time this paper was being written. However, all the engineering heavy lift planning and extensive dynamic analyses were performed for this plan and are described below.

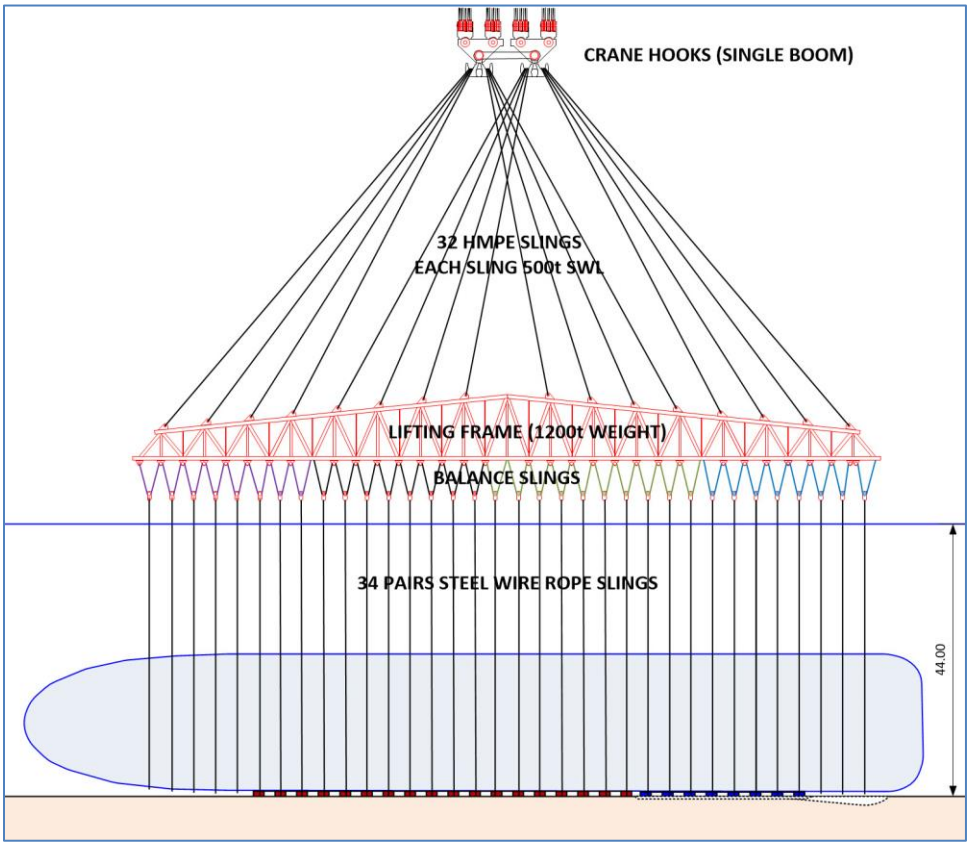

Figure 7 – Salvage Stage 2A, Rig Main Lifting Frame Supported by HMPE Slings from Crane Hooks

The balance slings beneath the lift frame accommodate slight differences in the lengths of the steel slings supporting the Sewol. The balance slings also ensure good load sharing between the steel slings.

The plan has no provision for length adjustment of the upper 32 HMPE slings. Hence the tolerance on their manufactured lengths was kept very tight (better than +/- 100mm over 70m length achieved).

The side lift takes the Sewol from the seabed to a position where it is approximately 30% emerged. It is then moved over a partly submerged vessel for subsequent raising above the water surface. Various vessels for the final stage of raising were considered. The following figures illustrate the option considered with a modified floating drydock.

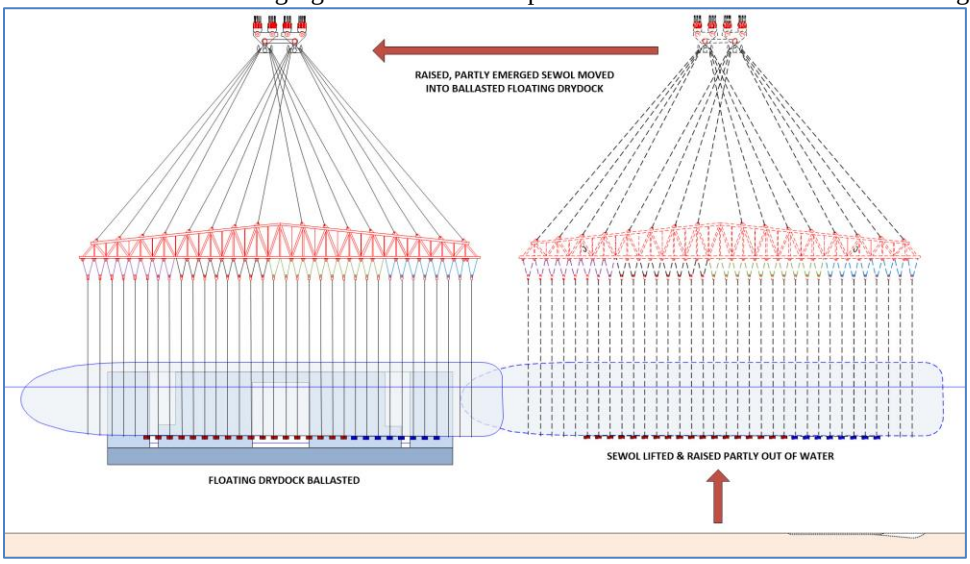

Figure 8 – Salvage Stage 2B and Stage 3A, Raise Sewol From Seabed and Move Over Submerged Floating Drydock

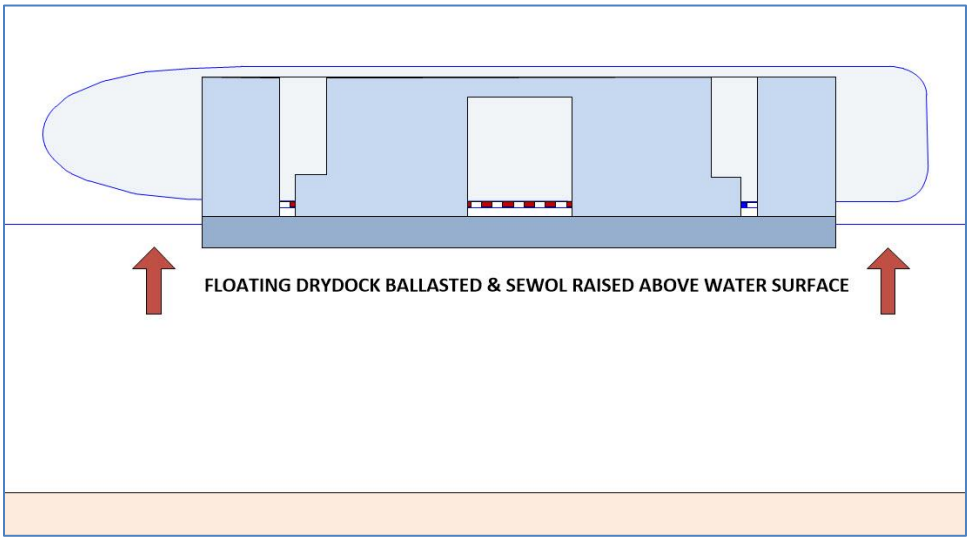

Figure 9 – Salvage Stage 3B, Deballast Drydock and Raise Sewol Above Water Surface

Once the drydock is deballasted to the target draft and the Sewol is above the water surface, the vessel is secured for a short ocean tow in relatively sheltered waters. Once at the target destination (Mokpo, Korea, at the time of writing) the Sewol will be offloaded using a SPMT (self-propelled modular transporter) system.

First Bow Lift

The first attempt at the bow lift occurred in mid-June, 2016. The buoyancy was not configured to ensure that the two crane hooks could be successfully used to control heeling. The effects of vessel dynamics were underestimated by the contractor and the bow slings cut 7m into the hull. The hull also heeled significantly as the bow was raised. The lift operation was stopped and the bow was set back down on the seabed without inserting any lifting beams. Further information on the failure of the first bow lift is given later (see also Figure 27).

Maximum trim reached 2.81° at around 750 minutes. The heel reached its maximum value of 2.0° around the same time. The port aft superstructure contact with the seabed was almost certainly the main thing limiting the heel. When the vessel was set back down the heel and trim returned to near zero, the same as before the lift.

It was found that no edge reinforcement had been placed (although it had been discussed and designed) between the slings and the deck edge where the tears occurred.

Second Bow Lift

The second bow lift occurred in the last days of July, 2016. The deck edge was fitted with a protector, although the tears made during the first lift were not repaired. The buoyancy arrangement was still not as recommended by the authors. The 5° target in trim was reached, but heel reached nearly 4° and space for insertion of the first set of lifting beams was very tight.

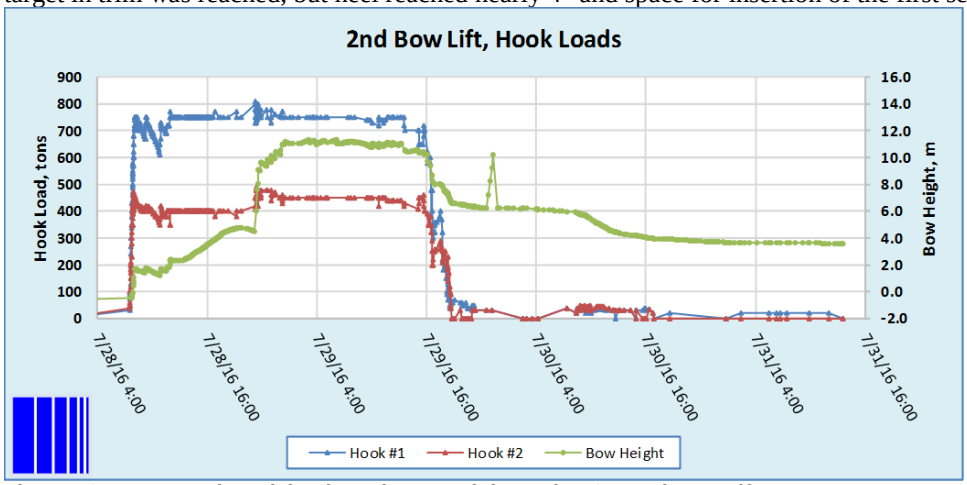

Figure 10 – Measured Hook loads and Bow Height During Second Bow Lift

The 2,500t capacity crane barge Dalihao was used for the bow lifts. Each of the two 1,200t main hooks were employed. The bow sling arrangement is described later.

In Figure 11 it is seen that when the target maximum heel of 5° is reached, at around 22:00 on July 28th, the hook loads are around 750t and 450t.

The first set of lifting beams were placed beneath the raised forward end of the Sewol between 4:00 and 16:00 on July 29th, before the bow was lowered. The hook loads are seen to reduce to low values after 16:00 on July 29th. However, the bow height and trim records show significant changes in value between 4:00 and 16:00 on the 30th as the additional buoyancy is modified such that the Sewol is made relatively heavier in water at the bow end. This change in buoyancy was planned to cause the hull to become stable and level on the lifting beams with the stern now raised off the seabed, as shown in Figure 6.

Unfortunately, as seen in Figure 11, the trim stabilized at 1.8° and the heel at -3.0° (instrument reading initially 0.7° making heel total change 3.7°).

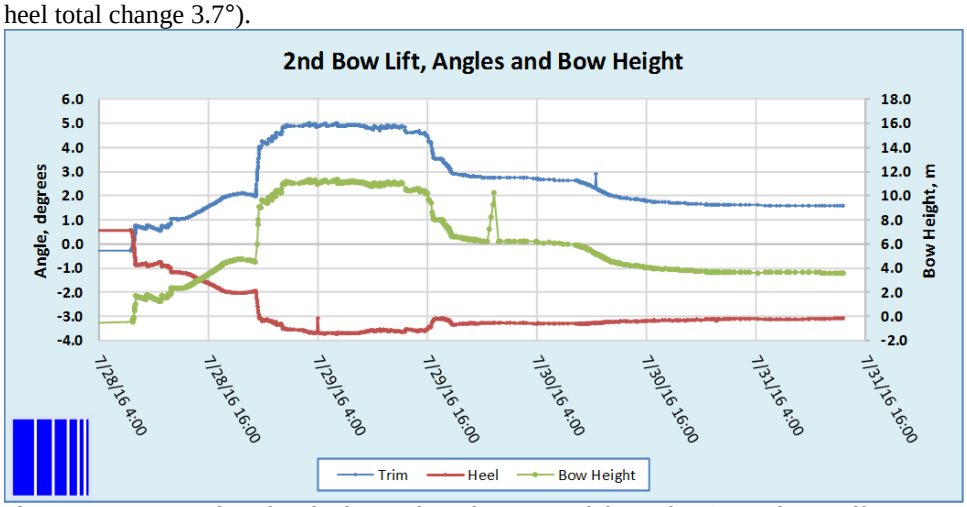

Figure 11 – Measured Heel and Trim Angles, plus Bow Height During Second Bow Lift

Aft Lifting Beam Installation Difficulties

Following the set down of the bow on the forward lifting beams and the redistribution of added ballast, the clearance between the seabed and the aft portion of the hull was less than expected. The attitude of the Sewol hull, now with significant trim and heel angles, was such that the stern port side was buried deeper into the seabed than had been hoped.

The next five months were spent attempting to insert the remaining 8 lifting beams. This paper explains more about the lessons learned. It is first important to understand the critical engineering calculations that went into the planning.

Bow Slings

The sling arrangement for the bow lift are shown schematically in Figure 12. Slings 1 and 2 are each made up with doubled 106mm steel wires shackled to form a continuous sling with four parts. Slings 3 and 4 are also make up a single continuous 4-part sling with each part being 106mm steel wire.

The two main hooks of the Dalihao have independent control and digital load indicators. All hook load data is logged by hand. No continuous data stream is recorded.

The slings are rigged such that the crane hooks each take a load that is inversely proportional to the horizontal distance from the transverse center of the total weight supported by the two hooks. If one hook is directly above the center of weight, the other will take no load. This can be inferred from the section view on the left side of Figure 12. However, as is also seen in Figure 12, the longitudinal locations of the slings are about 12m apart. Hence the relative loads shared by the hooks is expected to vary during the lift.

Sling Slippage and Vessel Heeling Moment

Although the slings have tight radii at some vessel edges, sling slippage is possible. The heeling moments that can be resisted by the slings are a function of the reactions at the load points and a coefficient of friction. The contractor estimated a coefficient of friction of 0.1 from previous experience.

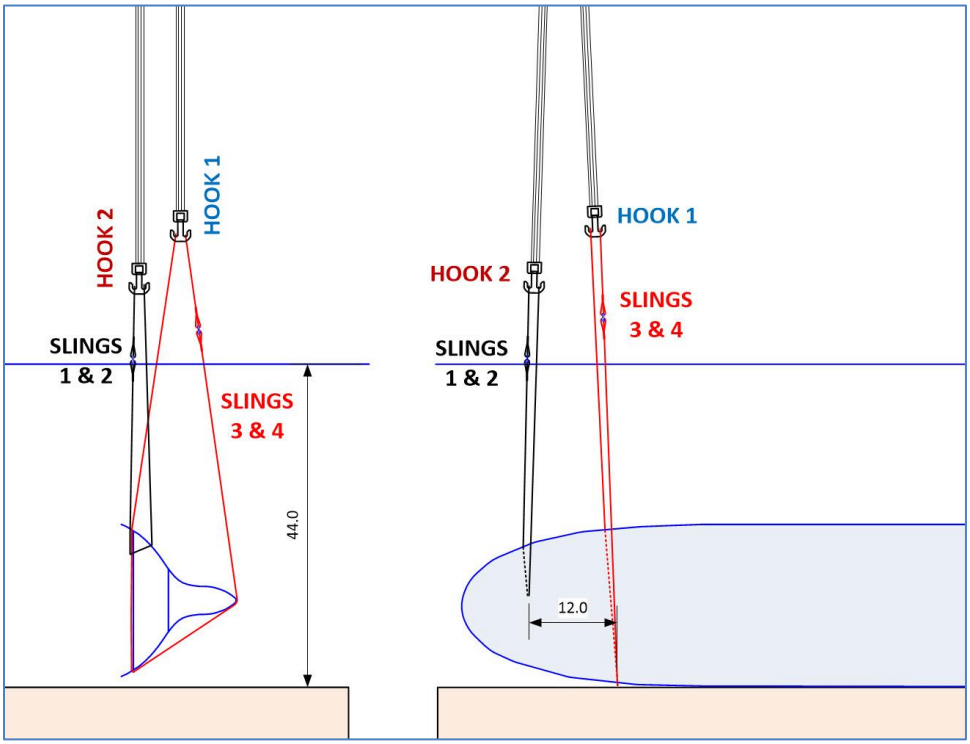

Figure 12 – Bow Sling Arrangements

Calculating Static Sling Loads from Longitudinal Force Balance

This is a simple calculation, but must assume a location for the longitudinal center of the ground reaction force.

Calculating Static Sling Loads from Transverse Force Balance

This calculation is simplified by assuming no heeling moment is taken by the ground reaction and that the hook loads will resist heeling as the hooks are raised.

Arrangement of Additional Buoyancy for Bow Lift

The additional buoyancy planned for the bow lift had to be sufficient to enable the bow to be raised without causing structural damage to the hull. The main structural constraints of concern were global and local buckling of the vessel plates and frames. A distribution of buoyancy along the length of the vessel and across the width and height of the vessel was made. The total additional buoyancy and its center were constantly tracked and monitored by diver surveys.

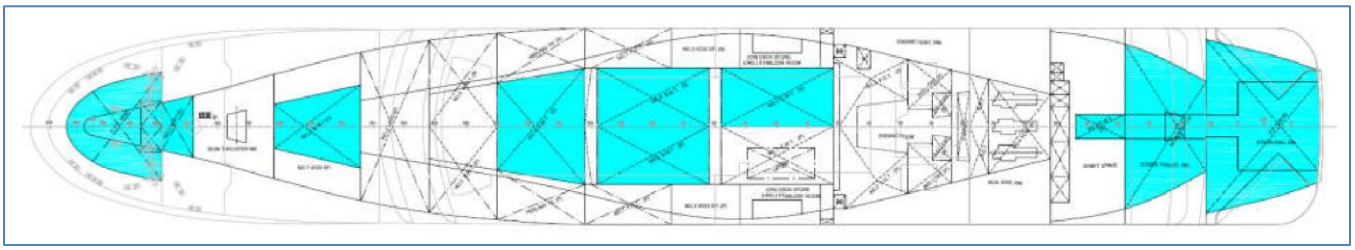

Figure 13 – Available Ships Tanks for Air-Filling, Total Useable 1,210t

Considerable time was taken in testing the ability of existing tanks to hold air and to make repairs on some.

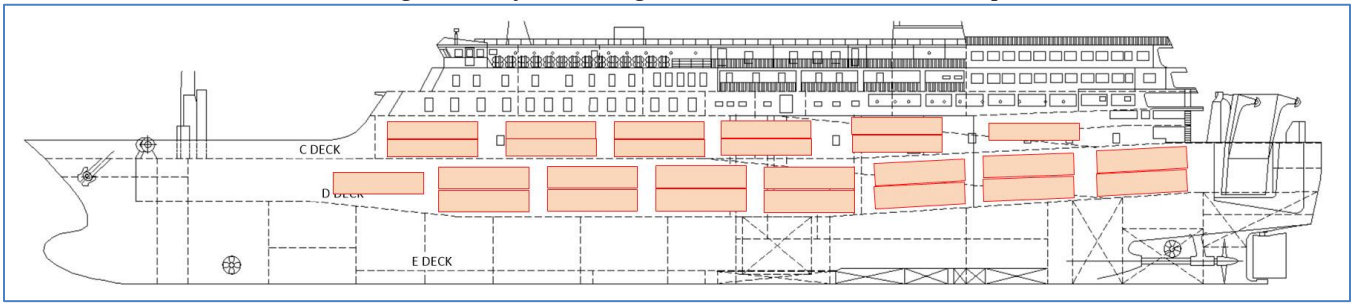

Figure 14 – Air Bags Added Inside Starboard Side on C-Deck and D-Deck, 30t to 54t each

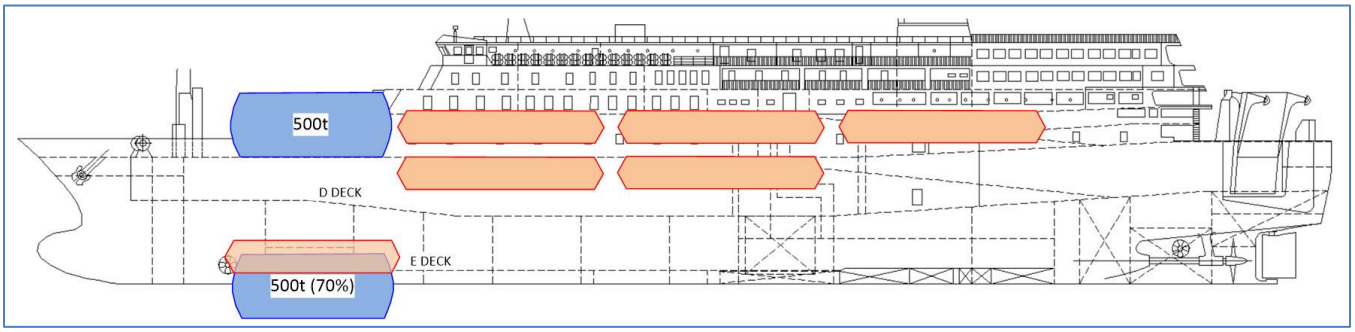

Figure 15 – External Buoyancy Pontoons, 500t Steel and 165t to 200t Rubber

Because of the high currents during spring tides, the external rubber pontoons were only installed when all other preparations for the lift were in place.

Bow Mooring

The current at the site has a peak velocity of over 3 knots (1.5 m/s) during spring tides and flows perpendicular to the wreck. To prevent the bow swinging laterally in the current during the bow lift, a pair of mooring lines were attached near the bow. Concrete gravity anchors were used with a bespoke 300t chain tensioner on the seabed, 102mm chain and 106mm wire. The anchors were placed in shallow pits approximately 400m on either side of the Sewol bow.

At the target bow lift height, the mooring system adds about 60t load to the bow slings. The mooring lines also apply a heeling moment to the vessel as they are attached at different elevations. The attachment is 10m higher on the keel side than on the topside. A typical heeling moment of 1,000 t-m is achieved during the bow lift. This moment tends to rotate the keel downwards and has the effect of moving the transverse center of the ground reaction towards the keel. The transverse movement is roughly 0.3m caused by a 1,000 t-m mooring moment. This is a linear relationship.

Currents cause a change in the mooring moment. A 2-knot (1.0m/s) from the topside induces a moment contributing to the mooring moment and a little over twice its value, at 2,150 t-m. A current from the keel direction induces a moment opposing the mooring moment.

Static Sling Force, Ground Force and Moment Equilibrium Calculation

To achieve a bow lift without the Sewol heeling, the upwards vertical forces from the slings, FG, the ground reaction and the buoyancy must balance the weight force from the vessel without causing a moment about the longitudinal axis. The calculation is complicated by the uncertainty of the ground reaction pressure distribution on the aft end of the vessel. The hull is on its side and the area in contact with the soil changes as the bow is raised. A method was developed to determine the longitudinal center of this area based on the ultimate bearing capacity of the soil, a simplified hull geometry and the bow lift angle. The total hook load is then solved based on the longitudinal force centers of the slings, the total weight, the additional buoyancy and the ground reaction. This method was implemented in Excel.

Having found the total hook load, the individual sling loads are determined by the user specifying one value and allowing the Excel app to solve equilibrium for the new case. Iterative calculation is needed as the longitudinal center of FG changes with the relative hook loads. This is because the slings and hooks are at different longitudinal locations.

At this point the Excel app has also solved for a transverse center of FG that will result in a zero-heeling moment. The mooring moment is also included within the equilibrium solution.

The engineer is then faced with the question of whether the lateral center of FG will result in a soil pressure distribution that is acceptable and will not result in the vessel heeling during the lift. The Excel app produces a diagram of the soil pressure beneath a cross section of the stern.

Seabed Soil Ultimate Bearing Pressures Considered for Bow Lift

Geotechnical issues are described in more detail later in this paper. It is useful at this point to consider the range of soil strengths considered for the planning of the bow lift.

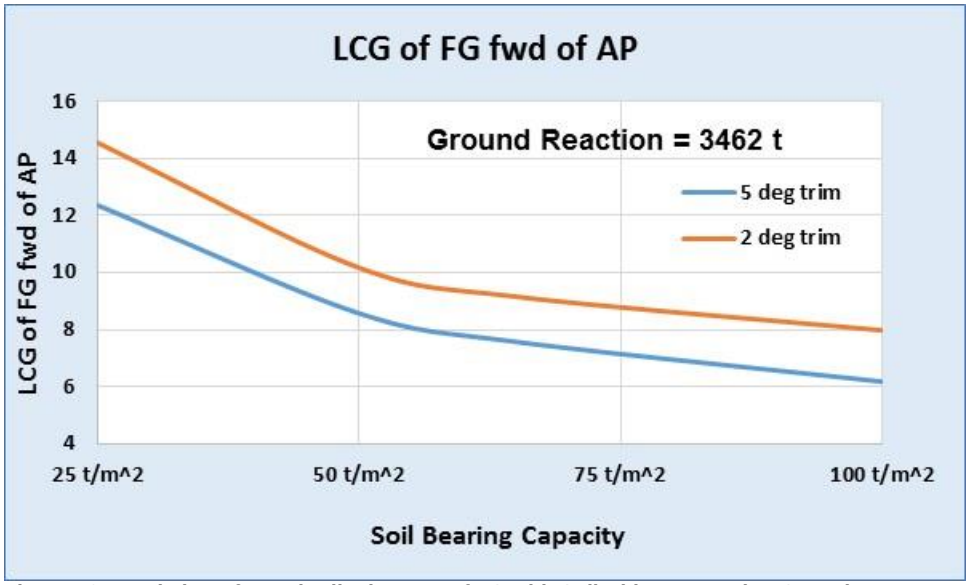

Figure 16 – Variation of Longitudinal center of FG with Soil Ultimate Bearing Capacity at Two Trim Angles

Conditions During Second Bow Lift

The measured hook loads exceed the predicted hook loads during the second bow lift. The difference is around 120t larger than expected. In the first bow lift a smaller, but similar difference was attributed to loss of air in the air bags and to a slight error in one of the large external pontoons. In this paper the assumed efficiency of the air bags and all external rubber pontoons has been reduced so that the total hook loads are correctly predicted. The summary load case results are given in the tables below.

Load Condition Before Buoyancy Additions				STA OTC 2017			
Item	**Weight**	**Lcg fr.AP**	**Lmom**	**Tcg fr.BL.**	**Tmom**	**Vcg Seabed**	**Vmom**
Light weight	6213 t	53.13 m	330098	11.77 m	73127	11.00 m	68343
Cargo total - (properties can be varied)	2159 t	69.29 m	149625	9.46 m	20428	9.00 m	19435
Provision	4 t	38.56 m	154	22.50 m	90	11.00 m	44
Dwt Constant	166 t	29.04 m	4821	11.77 m	1954	11.00 m	1826
Inflow mud	249 t	59.87 m	14925	15.65 m	3901	10.00 m	2493
Lwt buoyancy	-800 t	53.13 m	-42504	11.77 m	-9416	11.00 m	-8800
Soil resistance	0 t	52.00 m	0	12.00 m	0	0.00 m	0
Weight on Seabed w/o mooring & buoyancy	7992 t	57.20 m	457119	11.27 m	90084	10.43 m	83341
Mooring Lines Vertical Load	60 t	118.70 m	7122	7.00 m	420	5.50 m	330
W, Total Weight w/Mooring Before Buoyancy	**8052 t**	**57.66 m**	464241	**11.24 m**	90504	**10.39 m**	83671
Load Condition After Buoyancy Additions	**Weight**	**Lcg fr.AP**	**Lmom**	**STA OTC 2017**			
Total Buoyancy from Selected Case	**-3498 t**	**82.30 m**	-287855	**10.67 m**	-37313	**18.02 m**	-63029
W, Weight on seabed	**4554 t**	**38.73 m**	176386	**11.68 m**	53192	**4.53 m**	20642

Table 1 – Load and Buoyancy Condition for Second Bow Lift

Sling Loads, Hook Loads, Ground Reaction & Buoyancy Condition				STA OTC 2017			
Specify Static Sling Tensions #1 and #5	**Weight**	**Lcg fr. FG**	**Lmom**	**Tcg fr.BL.**	**Tmom**	**VCG**	**Vmom**
W, Weight on seabed	**4553.9 t**	**30.262 m**	137808	**11.68 m**	53192	**4.53 m**	20642
1# Lifting Sling tension User-specified)	**-225.0 t**	122.33 m	-27524	13.26 m	-2984	**Hook 2**	**450 t**
2# Lifting Sling	**-225.0 t**	122.33 m	-27524	13.26 m	-2984		
3# Lifting Sling	**-373.4 t**	112.23 m	-41903	7.55 m	-2819	**Hook 1**	**747 t**
4# Lifting Sling	**-373.4 t**	109.43 m	-40857	7.55 m	-2819		
5# Lifting Sling	**0.0 t**	111.03 m	0	14.00 m	0	**Hook Aux**	**0 t**
F_{sling}, Bow Lifting Force (total hook load)	**-1197 t**	**115.15 m**	-137808	**9.70 m**	-11605	**FG w/mooring**	
Ground Reaction, FG (Tcg without mooring)	**-3357 t**	**8.47 m**		12.39 m	-41587	**Tpivot**	**12.09 m**

Table 2 – Resulting Static Sling Loads, Hook Loads and FG, Ground Reaction, Second Bow Lift.

From Table 2 it is seen that the user has specified 225t to be the static load in each of slings 1 and 2. Hence Hook 2 takes 450t. The Excel app calculates 747t to be taken by Hook1. This matches the observed 450t and 750t shown in Figure 10.

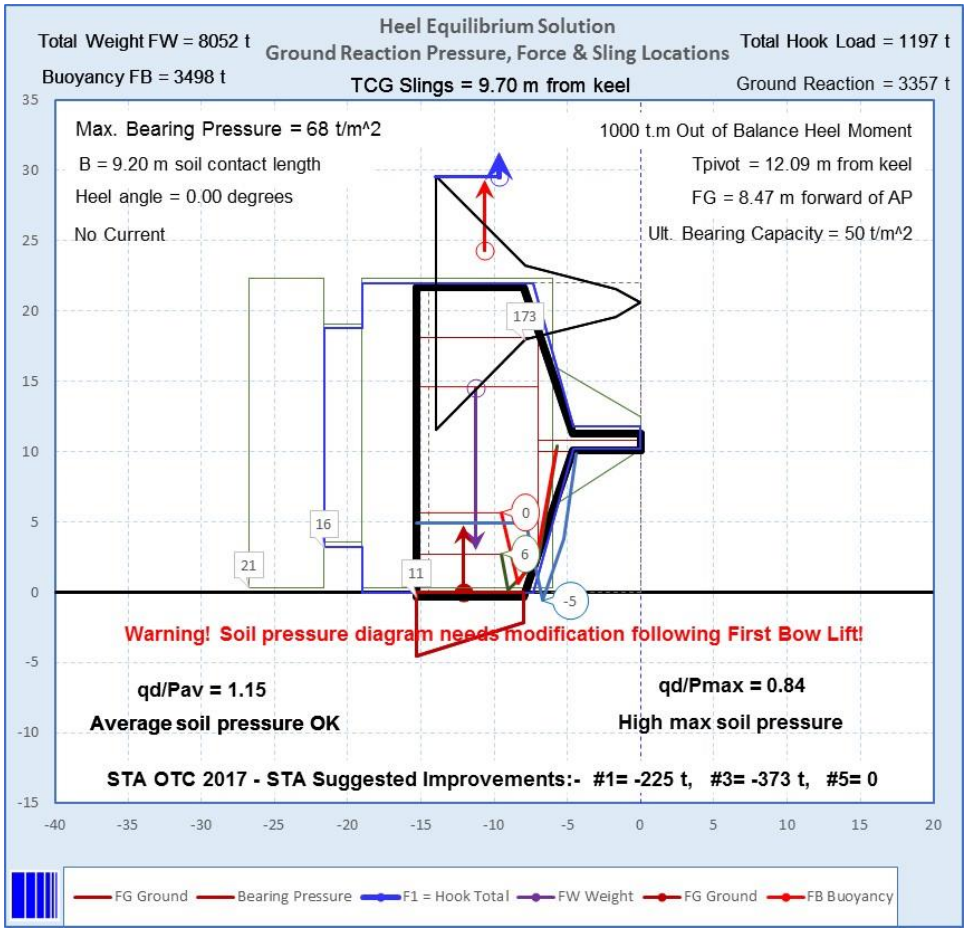

Figure 17 – Excel Chart Showing Sections at Frames, and Heel Equilibrium Solution for Second Bow Lift.

Labels indicate vessel frame numbers. Each frame identified is drawn with a different line color in the Excel chart. The frames are shown with the vessel trimmed. Hence Frame 173, in the region where the bow slings attach, appears raised. Frames 0, 6 and -5 are indicated and can be seen to be without any significant seabed contact.

The upper short blue arrow indicates the location and magnitude of the combined sling loads. The upper red arrow indicates the location and magnitude of the combined added buoyancy force. The central purple arrow, pointing down, indicates the location and magnitude of the combined weight force. The lower brown arrow indicates the location and magnitude of FG, the ground reaction force. The variable Tpivot, is the transverse distance of FG from the keel. At this distance, FG causes a moment that balances the system such that there is no net heeling moment.

The brown trapezoidal area beneath the seabed indicates the reaction pressure that would provide the force FG, if applied over the area of hull calculated to be in contact with the seabed in this load condition.

Figure 17 contains a red warning that the soil pressure diagram needs modification following the first bow lift. This is because the vessel heeled (topside going down) during the first bow lift and will have left an indented and disturbed area of soil. Heeling in the same direction would have less resistance from the soil during a second bow lift.

Numerous other data are listed on Figure 17, enabling the Excel app to be a useful tool to investigate alternative buoyancy arrangements and potential sling alternatives. For example, the soil ultimate bearing capacity used in the above results chart is 50 t/m^2.

Dynamic Analysis Considerations

In many heavy lift operations, the loads to be lifted remain above water. In this salvage operation, the load to be lifted starts fully submerged and has a lightship mass of a little over 6,000t. With cargo and other items, as shown in Table 1, the weight in water is around 8,000t. Additional buoyancy can significantly reduce the weight to be lifted. However, the mass of "trapped" water inside the vessel and the effect of added mass of water around the vessel must be considered in dynamic response calculations. These additional sources of mass increase the total submerged structural mass of the Sewol, for dynamic analysis calculations, by more than a factor of ten.

The hydrodynamic analysis of the SEWOL vessel is an extreme case since the vessel is laying on the seabed and hence part of the vessel is non-diffracting. The effect of numerical integration of the finite depth Green function for panels so close to the seabed is also not quantified and is a source of inaccuracy. Additionally, as the name suggests, the potential flow method does

not consider any viscous flow effects. These limitations must be kept in mind when using the results. Experienced judgment is needed.

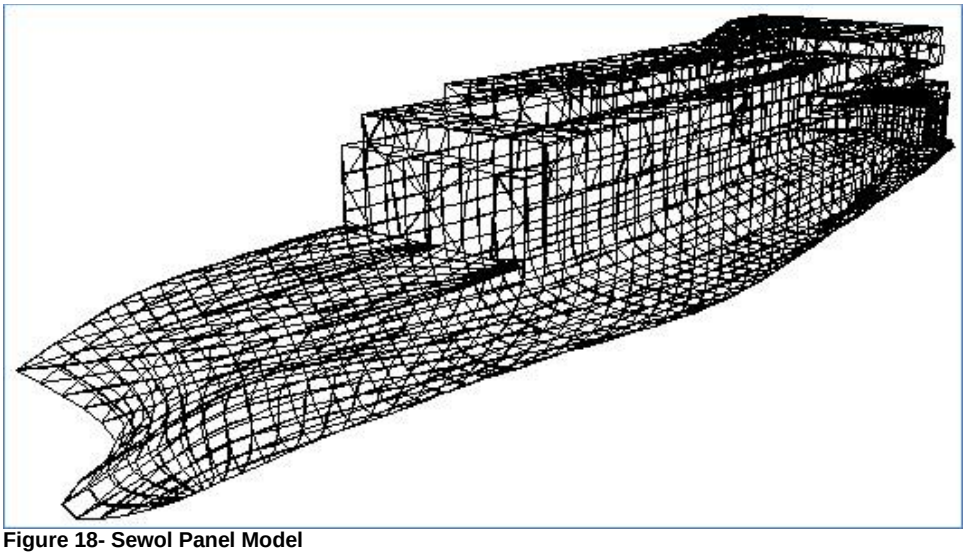

Figure 18- Sewol Panel Model

Trapped Water Mass

The total displaced volume by the ship is obtained from the panel model as shown in Figure 18, which is 51,328 m^3 and equivalent to 52,611t (approximating internal structures and machinery to occupy relatively insignificant volume). This mass compared to the lightship weight of around 8,000t has significant effect on the dynamics load on the cranes.

Added Hydrodynamic Mass

The additional force required to move a body under water is generally quantified as the added mass while solving the equation of motion. This apparent mass is a wave frequency dependent quantity and obtained through potential flow analysis. To understand the sensitivity towards the depth of submergence, and the pitch angle, several analyses are performed. First, the vessel is kept at various depths (vessel origin at 17m, 22m, 27m and 33m) and the added mass is calculated as shown in Figure 19. Secondly, the vessel is kept at different pitch angle, as the heavy lift involved lifting the vessel by the bow, and the added mass variation is obtained as shown in Figure 20. As the vessel is closer to the water surface, it radiates more waves and hence we see a higher variation in the added mass. It could be seen that a heave added mass of more than 60,000t on average and as high as over 100,000t is observed.

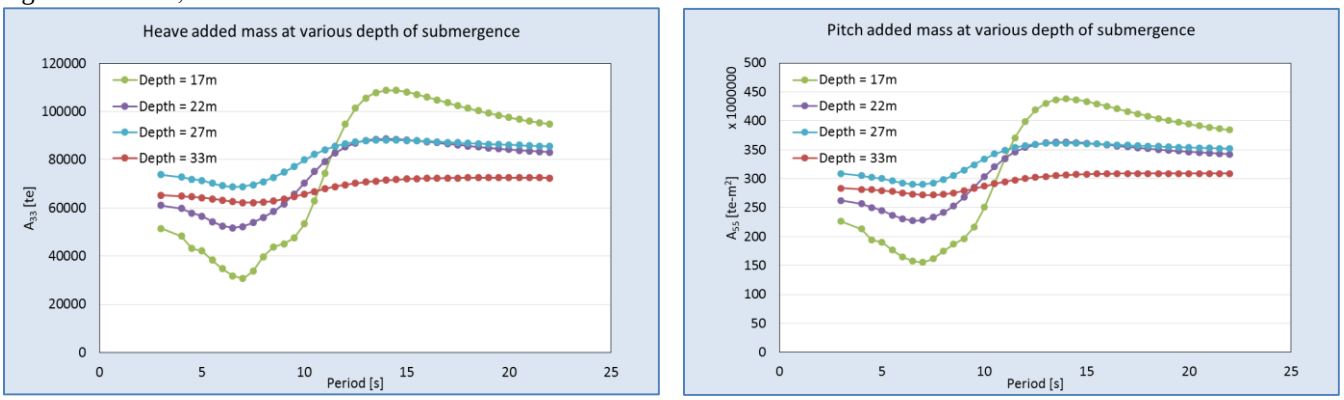

Figure 19 - Heave and Pitch Added Mass of Sewol at Various Depths of Submergence

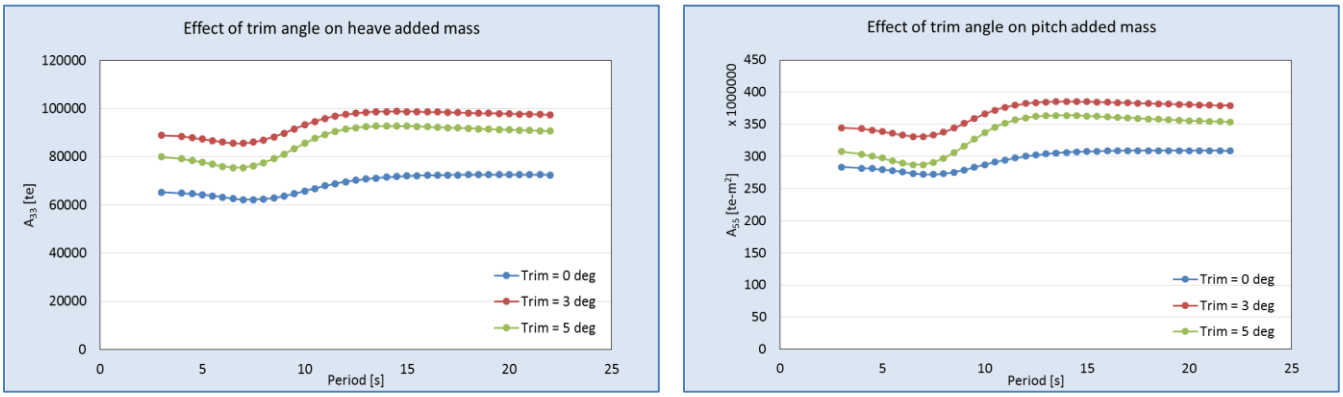

Figure 20 - Effect of Sewol Trim on Heave and Pitch Added Mass

OrcaFlex Model of Bow Lift

OrcaFlex was used to predict dynamic sling tensions under a range of potential operating conditions. The models developed used fully coupled analysis with the motions of the Dalihao crane barge being driven by diffraction force RAOs and influenced by the crane hook loads through appropriately modeled sling systems to the submerged Sewol model. Simultaneously, the Sewol model was driven with diffraction force RAOs and was given a seabed ground reaction as well as sling loads from the crane barge. The seabed interface permitted the Sewol to respond in pitch and roll.

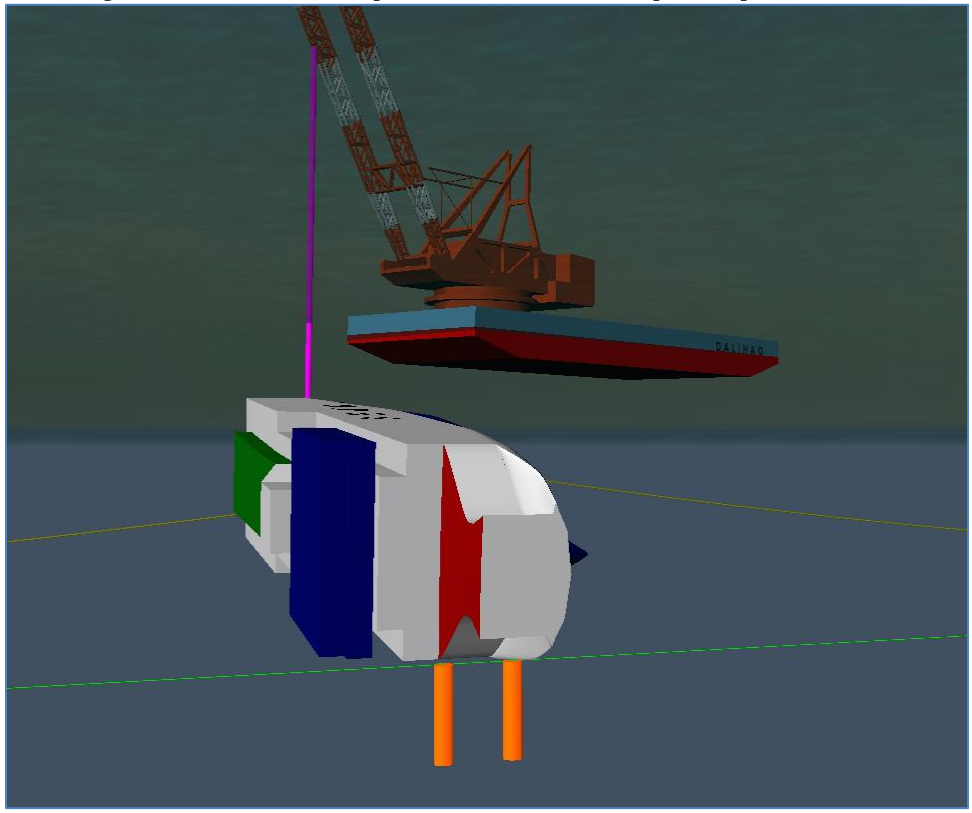

Figure 21 – OrcaFlex Shaded Graphics View Showing Seabed Reaction Model

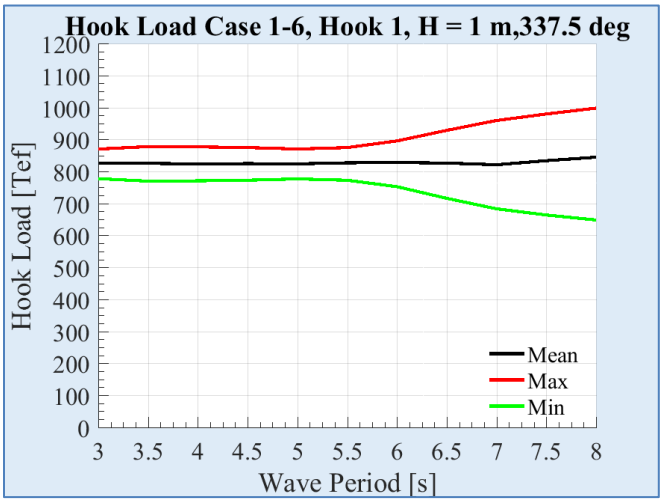

Figure 22 – Example of Dynamic Response Variation of Hook Loads with Wave Period

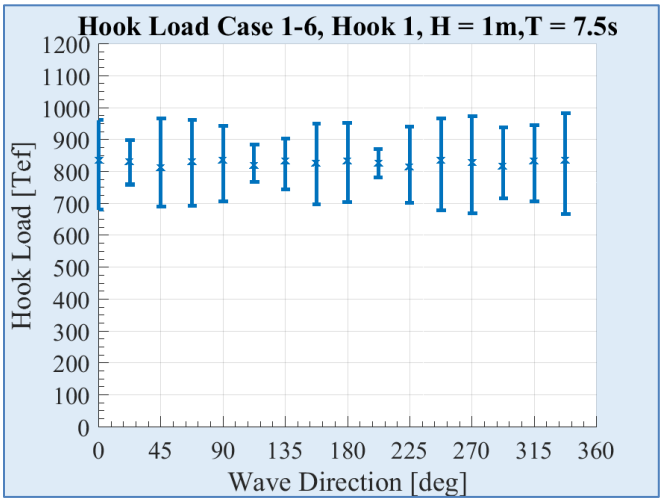

Figure 23 – Example of Dynamic Response Variation of Hook Loads with Wave Attack Angle

OrcaFlex Model Ground Reaction During One Wave Cycle

The ground reaction is simulated with the two non-linear soil springs previously described. During passage of a wave the reactions vary. If the wave is in the beam direction relative to the Sewol, the hydrodynamic loads cause a heeling moment and the soil on the keel side becomes more heavily loaded as the soil on the deck side becomes less loaded during one half of the wave cycle. The loading reverses during the next half of the cycle. This is illustrated below.

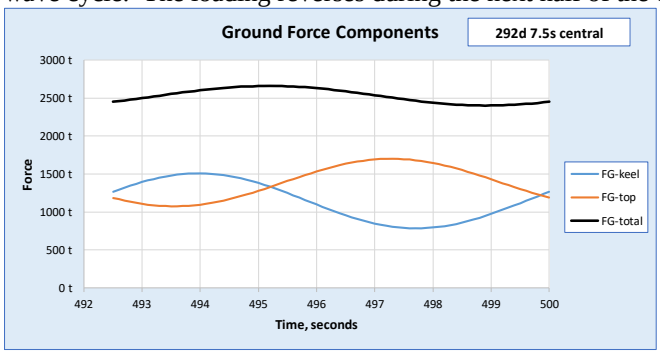

Figure 24 – OrcaFlex Soil Spring Forces during a wave cycle, 1m wave height, 7.5-sec period

The variation of the total soil reaction, FG-total, is shown by the upper black line in Figure 24. The sum of the two soil spring forces, FG-top and FG-keel, equals FG.

The dynamic load variation in FG-total is not necessarily in phase with the dynamic sling load variation as the wave passes by. This is illustrated below.

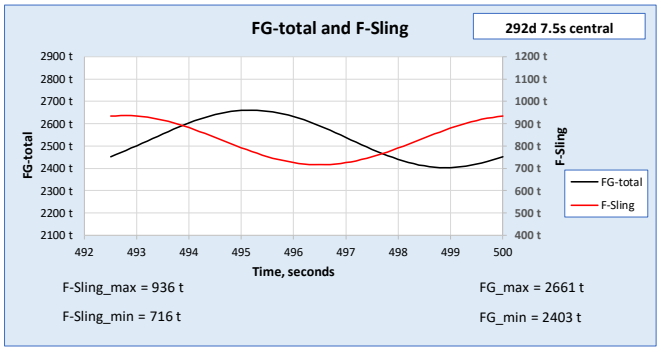

Figure 25 - Example of Ground Reaction and Sling Tension Variation during a Wave Cycle

The sling tension is seen to reach a maximum value at around the end of the wave cycle, while the ground reaction reaches a maximum one quarter way through the cycle.

In this example the wave direction is 292.5 degrees. This is almost beam-on to the Sewol.

The phasing of the sling tension time history and the ground reaction time history is influenced by the motions (mostly vertical) of the Dalihao crane boom tip and by the wave diffraction forces and moments on the Sewol.

The soil spring forces are converted to soil pressures in the next figure. Only the peak values are shown during the wave cycle. These occur when the heeling moment is at its maximum and at its minimum value.

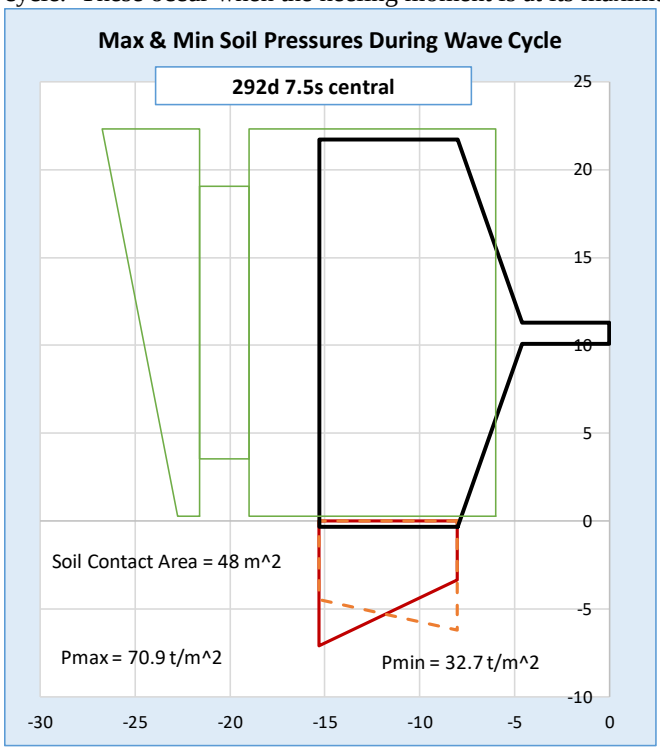

Figure 26 - Example of Soil Pressure Variation During One Wave Cycle

Predicting Dynamic Sling Tensions for Bow Lift Using Wave Forecasts

Dynamic sling tensions during the Bow lift are not significantly influenced by wind or current, if the bow mooring system prevents the bow from having large lateral offsets. Hence the prediction of waves is critical. The dynamic analysis work showed that waves greater than 1.0m significant height would be acceptable, at periods less than 7 seconds. At longer periods, sling tension dynamic amplifications would be undesirably large.

First Bow Lift

At the time of the first bow lift, daily weather forecasts were being obtained from two sources, Offshore Weather Services Pty Ltd., Australia (OWS) and Buoyweather, USA (BW), each providing wind and wave predictions for up to 5 days ahead. The forecasts from the day before the first bow lift are compared below.

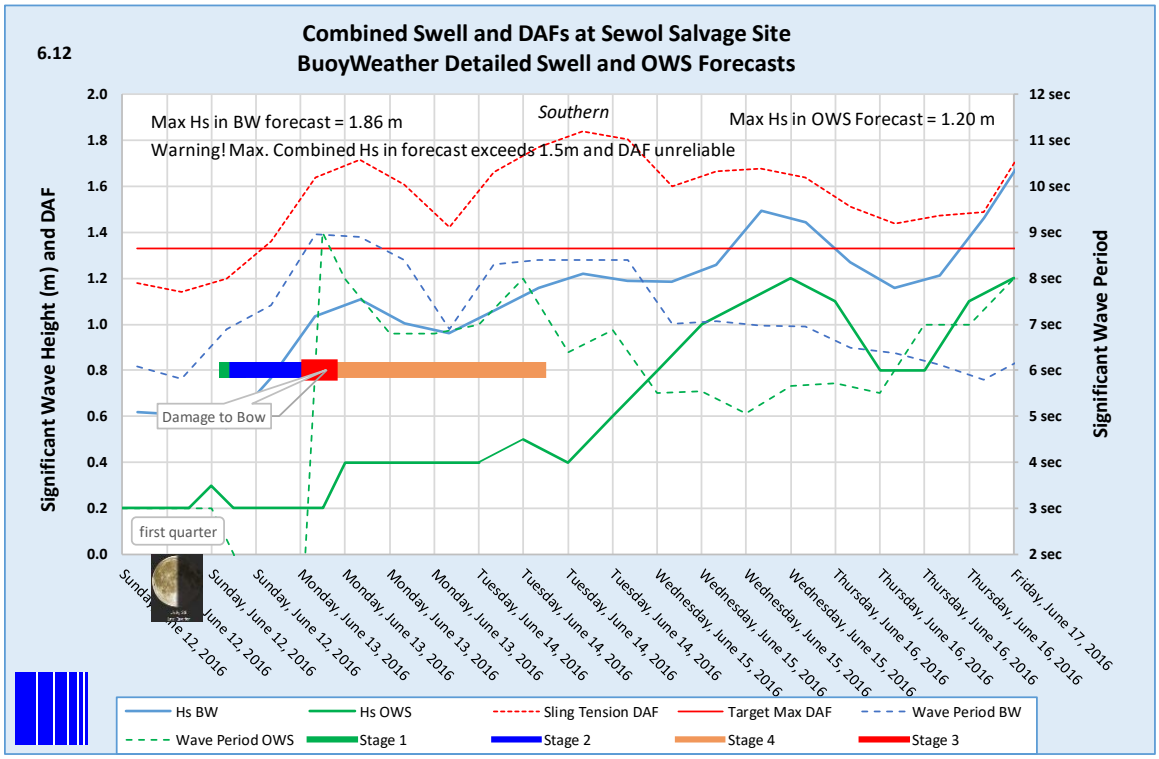

Figure 27 – Forecast Waves One Day Before and During First Bow Lift

The thick colored bar indicates the bow lift stages with the red portion indicating when the damage occurred, with the slings cutting into the bow.

The lower thin solid green line shows the wave heights forecast by OWS, with wave periods shown by the green broken line. The thin solid blue line indicates the wave heights forecast by BW, with wave periods shown by the blue broken line. The thin red horizontal line indicates a suggested maximum target for the maximum sling tension DAF. The red broken line at the top indicates the DAF calculated by the authors, based upon the most critical wave forecast (either OWS or BW).

It is seen that both forecasts indicate that the wave period was forecast to increase to 9 seconds at the same time on June 13th when the damage occurred to the bow. The salvage contractor reported suddenly increased wave heights (but not periods) around 1:30am on the 13th. The highest waves at this time were forecast by BW to be 1.0m to 1.1m. The longer wave period, resulting from swells coming into the area, would have caused the sling dynamic tensions to have increased to a DAF of around 1.6. This is roughly in line with the hook load variations logged during the first bow lift.

Prior to the lift the authors had warned that individual sling tensions are predicted to have DAF values of around 1.3 and 1.6 in 0.6m and 1.0m significant height waves with 8.0 seconds characteristic periods.

This implies that individual static sling loads will be increased by a factor of up to 1.6 in waves of 8 seconds period with significant height of 1.0 meters. This should be seen in the hook loads such that if a mean hook load (static value) is 500 tons, it will vary in the range from 300 tons minimum to 800 tons maximum, in these conditions.

Improved Forecasting for Second Bow Lift

KIOST were employed to provide both measure wave data and forecast wave data in preparation for the second bow lift. Wave measurements were made with a buoy about 2km from the salvage site and reported every hour via a continuously updated web site. The measured data enabled some short-term calibration of the three forecasts.

Within the few weeks of measured data, no reliable trends between the forecasts and measurements were determined. Generally during period of relatively small waves, all three forecasts showed reasonable agreement with measured data. On some occasions, larger (up to 1.8m significant) measured wave heights exceeded those predicted by 40% and vice versa. Similar disparities were seen in wave period forecasts and measurements.

Forecast and Measured Waves, Second Bow Lift

Figure 28 contains the comparison of three wave forecasts (updated every day) recorded waves and sling tension DAFs for the week of the second bow lift. All three forecasts predicted the waves to be diminishing in height and period in the day before the lift commenced. The measured wave heights, shown with the thicker black line, were most closely predicted by the KIOST forecasts indicated with solid brown. The other two forecasts were low on the wave height but closer on measured wave period, indicates with dotted black line. KIOST slightly over-estimated wave periods during the lift. Note the sudden large increase in measured wave period on August 2nd, after the lift.

The sling tension DAF values calculated using the measured waves are shown with the thin solid black line. The values vary from 1.0 to 1.2 during the lift period beginning on the 28th and ending on the 30th. DAFs predicted by the forecasts during the lift period reach 1.3 (KIOST). The other two do not go above 1.1.

In terms of dynamic predictions, the second bow lift can be regarded as successful. However, the heeling was not controlled as it should have been, resulting in long delays to the project.

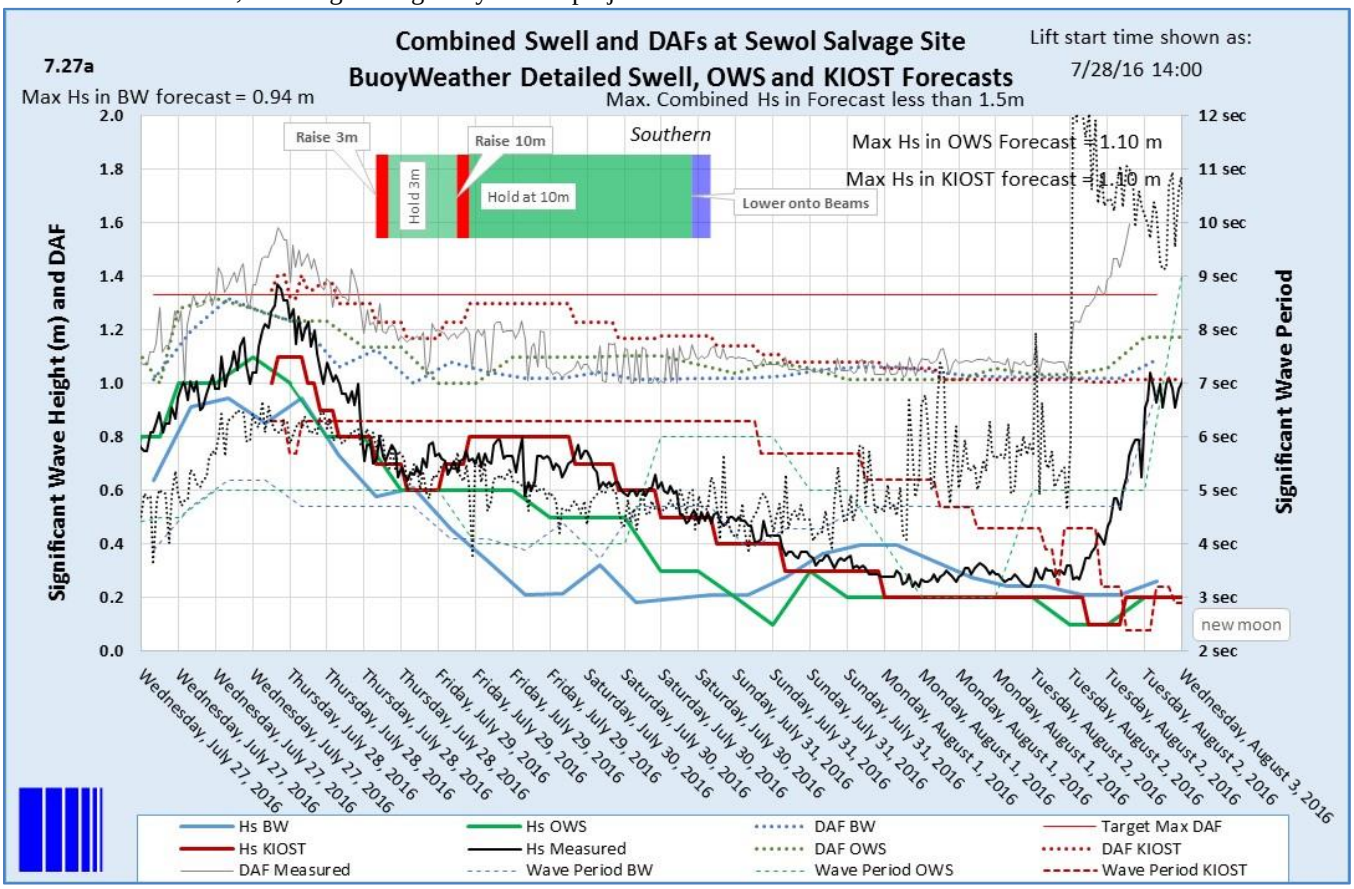

Figure 28 - Forecast and Measured Waves and Sling DAFs, Second Bow Lift

Side Lift Planning and Analysis

The Sewol hydrodynamic model described previously was used in various evolutions of OrcaFlex models, accommodating changes in buoyancy plans, changes in the main lift frame and changes in the HMPE slings as the project evolved. The final system analyzed is shown in Figure 29. This dynamic analysis had many challenges. Like the bow lift, the system involves large vessels coupled through the spring system of the rigging. There are three large rigid bodies:

- 12,000t lift crane barge, 230,000t displacement
- 1,200t main lifting frame
- Sewol with additional buoyancy, approximately 6,000t suspended weight, depending on load case.

The crane barge behaves like a ship and has conventional added mass and diffraction force characteristics. It's trim and dynamic behavior are significantly influenced by the suspended Sewol and lifting frame. The lifting frame remains above water and has no added mass complications. The Sewol has diffraction and added mass characteristics that vary significantly with its depth of submergence (see Figure 19). Because of this a different OrcaFlex model is used for four discreet depths considered during the side lift process. These correspond to the center of the hull being at depths of:

- 33m – on the seabed
- 27m – raised 6m
- 23m - raised 10m
- 17m – raised 16m (also has reduced buoyancy)

The upper HMPE slings are considered with two axial stiffness (AE) values. The first value, AE = 500MN is appropriate for their new condition and the second, AE = 1,000MN, is for the condition where they have become stiffer after repeated relatively high loading for several days. This latter condition could exist if the Sewol must remain suspended during unplanned rough conditions.

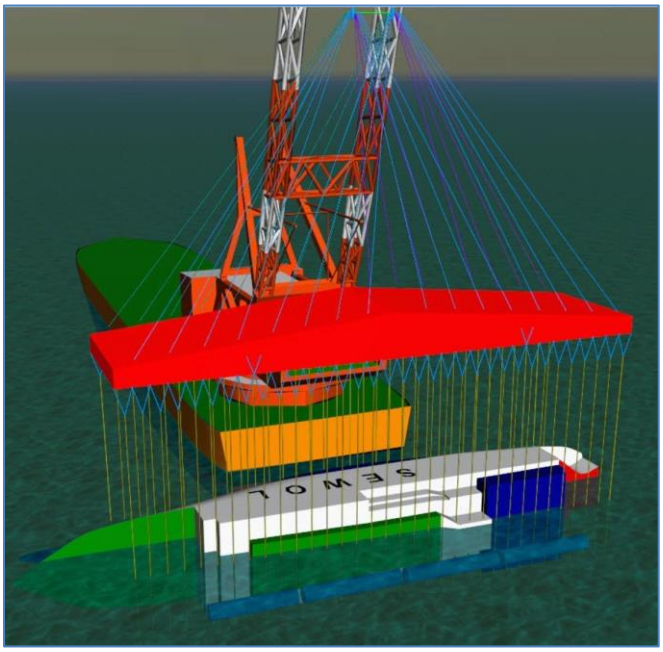

Figure 29 – OrcaFlex Model of System Side Lift Showing Sewol 30% Emerged

The dynamic responses of the system to waves is complex. There is a tendency for largest dynamic responses to occur at wave period beyond 8 seconds when the Sewol is submerged, but for larger dynamic responses in shorter waves when the Sewol is partly emerged. This is illustrated for one of the two main hook loads shown below for a 1m significant wave height approaching from the 180-degree direction (heading towards the bow of the Sewol and on the beam of the crane).

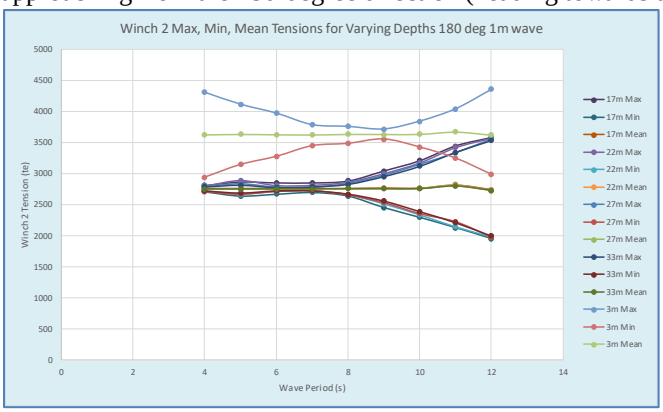

Figure 30 - Hook 2 Max, Min, Mean Hook Loads, Various Depths, AE=500MN, Waves 1m at 180 deg.

There is insufficient space in this paper to fully discuss the dynamic response observations made during the project. Some sample results for sling tensions are provided below.

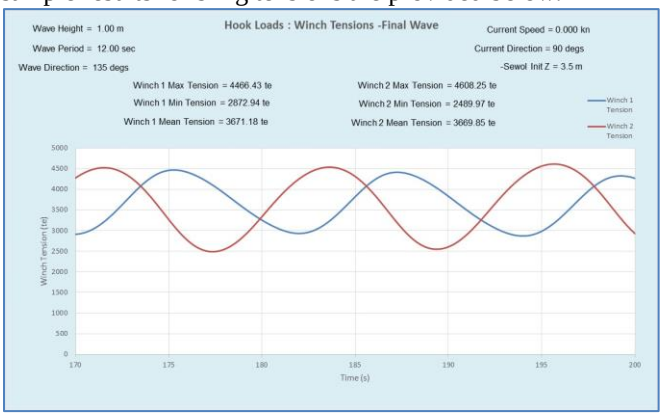

Figure 31 – Main Hook Loads, Sewol Depth 17m, AE=500MN, 1m Wave 135deg, T=12s

In Figure 31, it is seen that the load case results in the main hook load dynamic tension variations being nearly perfectly out of phase.

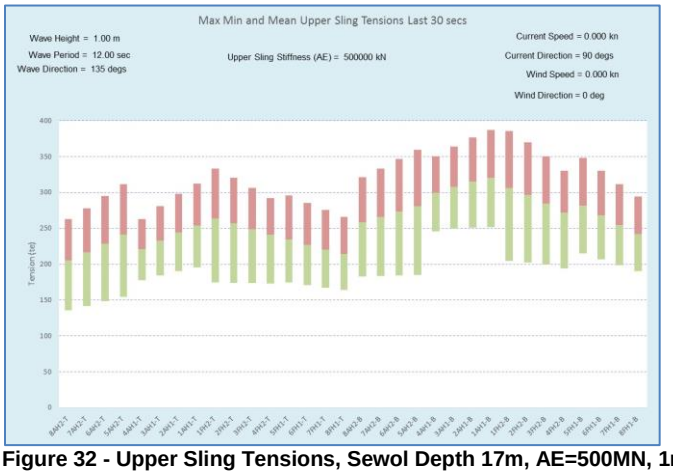

Figure 32 - Upper Sling Tensions, Sewol Depth 17m, AE=500MN, 1m Wave 135deg, T=12s

The maximum and minimum tensions in each of the upper HMPE slings are reported in Figure 32 for the same load case as in Figure 31. The balance sling maximum and minimum values for the same load case are reported in Figure 33.

Figure 33 - Balance Sling Tensions, Sewol Depth 17m, AE=500MN, 1m Wave 135deg, T=12s

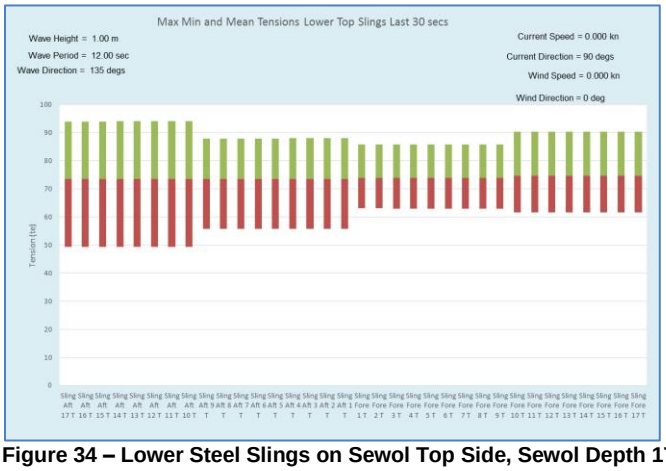

Figure 34 – Lower Steel Slings on Sewol Top Side, Sewol Depth 17m, AE=500MN, 1m Wave 135deg, T=12s

Figure 34 shows the maximum and minimum tensions in the steel slings below the main lifting frame, on the Sewol topside, for the same load case as in Figure 31. The results for this load case for the steel slings on the keel side are shown in Figure 34.

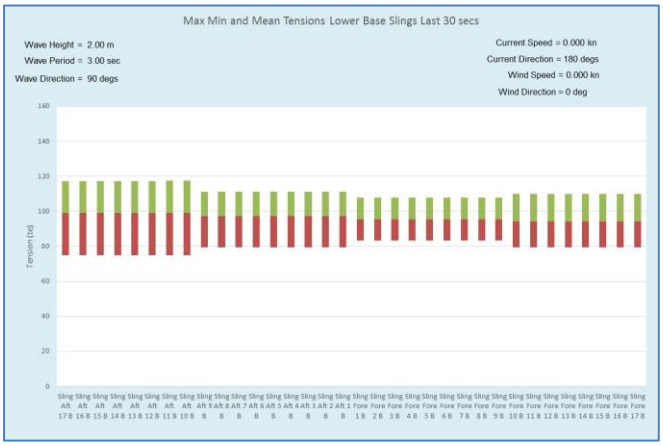

Figure 35 – Lower Steel Slings on Sewol Keel Side, Sewol Depth 17m, AE=500MN, 1m Wave 135deg, T=12s

For each load case analyzed, the motions of the three large rigid bodies are documented with time histories (to ensure that a steady-state response has been found) and with summary statistics.

Detailed Static and Dynamic Stress Analysis of Sewol Hull

For each critical static and dynamic load case for each of the bow and side lift conditions, ANSYS 17.0 was used to determine local stresses in the Sewol hull. Plate and stiffener buckling stress checks were implemented using DNV-RP-C201. ADPL scripts were used extensively for applying distributed and point buoyancy loads and distributing the mass.

The analysis identified limiting dynamic conditions and concluded that the bow lift, with the final buoyancy arrangement, could be made safely if dynamic responses are such that the sling tensions have DAFs not greater than 1.3. This roughly corresponds to waves with a significant height of less than 1 meter. Under these conditions the hull stresses will not result in a global buckling behavior.

The stern area in contact with the seabed will experience local damage if the seabed has a high bearing capacity. This would be the case with the upper bound 80 tons/m^2 considered by STA.

If the seabed has the lower bound bearing capacity of 30 tons/m^2 considered by STA, damage to the stern should be minimal.

Key buckling analysis results are summarized below:

- At regions other than the aft soil interaction region, the maximum hull plate buckling resistance utilization is 73% and this occurs at frame 81 for dynamic amplification factor (DAF) of 1.5.
- With the upper bound soil bearing pressure of 80 Te/m2, the hull plate, web stiffeners and longitudinal girder are expected to incur local buckling and deformation in the local soil contact area.
- With the lower bound soil bearing pressure of 30 Te/m^2, the hull plate, and longitudinal girder buckling resistance utilizations are acceptable.
- The maximum plate buckling utilization in superstructure plate is 113% and this occurs at frame 106 for dynamic amplification factor (DAF) of 1.5.

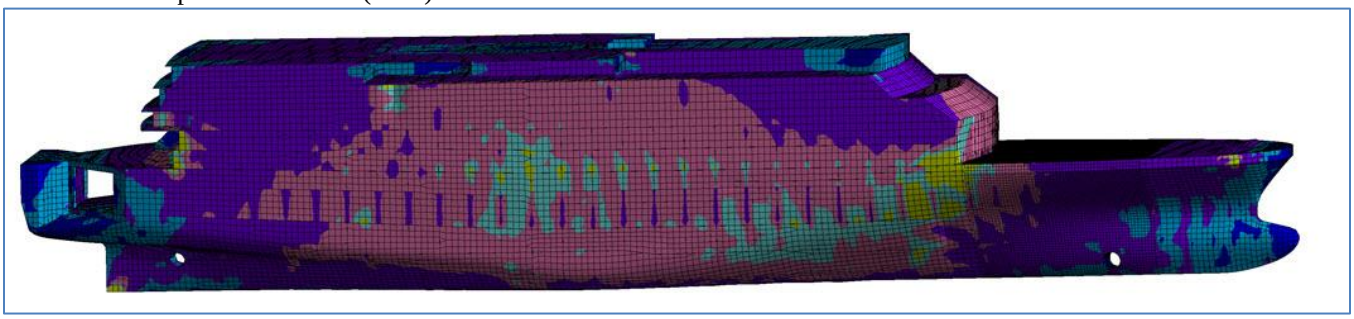

Figure 36 – ANSYS FE Model, Including Superstructure, Bow Lift Von Mises Stresses (no values shown)

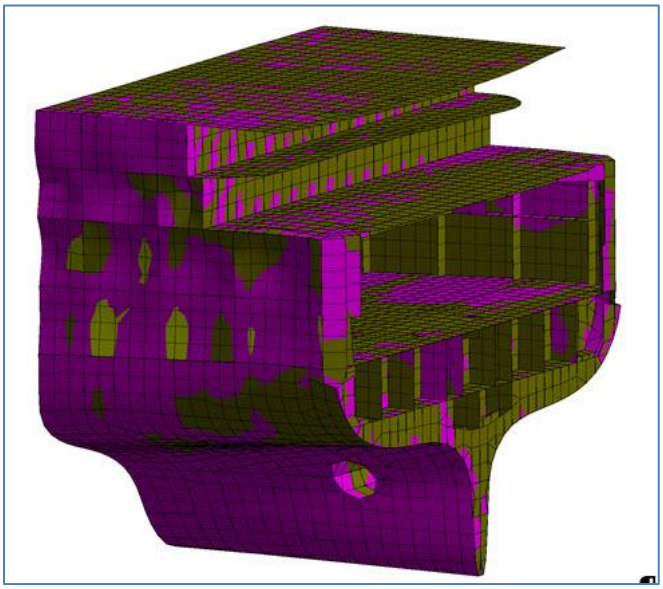

Figure 37 – ANSYS Model, Detail in Area of Ground Pressure

Geotechnical Background

Attention to geotechnical detail in considering the condition of the seabed relative to a wreck has rarely been an important factor in the mind of a salvage contractor, other than to note whether a vessel is on "the rocks", or partially submerged in soft mud.

Additionally, in the case of Sewol the wreck lay clearly proud of the mudline; and the salvage contractor's site investigation specialist had defined the sub-bottom as a simple two-layer system consisting of a dense (stiff) upper layer over a marginally weaker stratum about two metres below the upper layer.

In summary, these layers were characterised as follows:

I. Gravelly soil (medium dense to dense) cohesion 10 kPa, angle of internal friction 40°, and a notional allowable bearing capacity 700 kPa.

II. Residual soil ("cohesive with high shear strength") plasticity index 10.6, cohesion 50kPa, effective angle of internal friction 27°, and a notional allowable bearing capacity 350 kPa.

This interpretation proved not to be the case and ultimately this simple model with the expectations of a near surface dense seabed was a major contributor to delays and the failure to lift the wreck within the first year of the contract.

Site Investigation Overview

1) a comprehensive seabed survey incorporating side scan sonar, multi-beam sonar, sub-bottom profiler, drop coring and grab sampling. This was performed by the Korean Institute of Ocean Science and Technology (KIOST survey), made between 8/1/2015 and 29/1/2015 in two campaigns;
2) as 1) but more focused on the wreck site, and without the use of sub-bottom profiler or seabed sampling, performed by the Tianjin Survey and Design Institute for Water Transport and Engineering for SSC (TIWT survey), between 15/8/2015 and 29/8/2015; and
3) a geotechnical drilling investigation at eight locations near the wreck each extending to a depth approximately 4m below mudline, also performed by the Tianjin Institute (TIWT geotechnical investigation), between 17/8/2015 and 11/9/2015.

The results of 1) and 2) the KIOST and TIWT surveys were both comprehensive and consistent insofar as they portrayed a high-resolution definition of the wreck relative to the seabed (see Figure 38 and Figure 39 as examples). These example images were a small part of about 20 line kilometres of Multi-beam survey from the TWIT survey 500m by 1000m target site, and more than 75 line kilometres of similar survey run concurrently with Chirp and Sparker sub-bottom profilers over an overlapping 2 by 2, and a 2.3 by 1, kilometre target area from the KIOST survey.

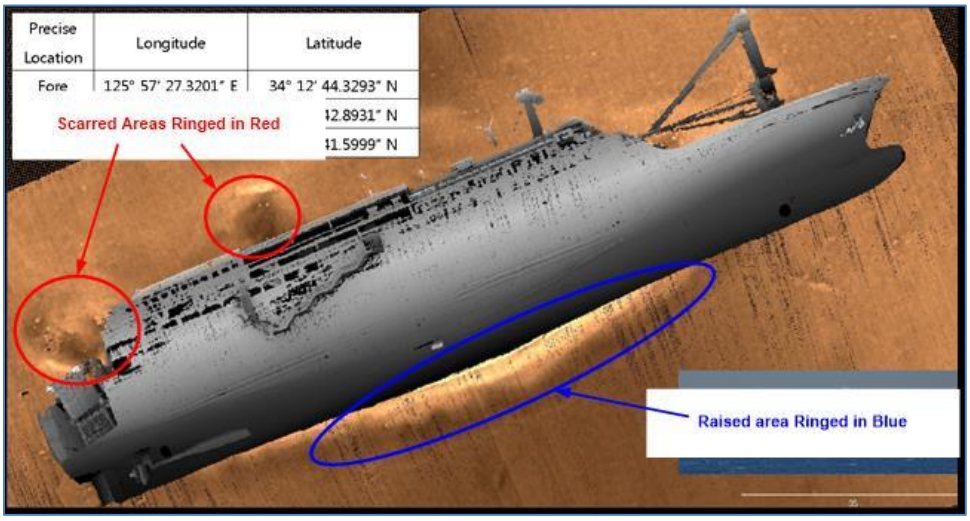

Figure 38 – Scan from KIOST with Areas of Special Interest Indicated

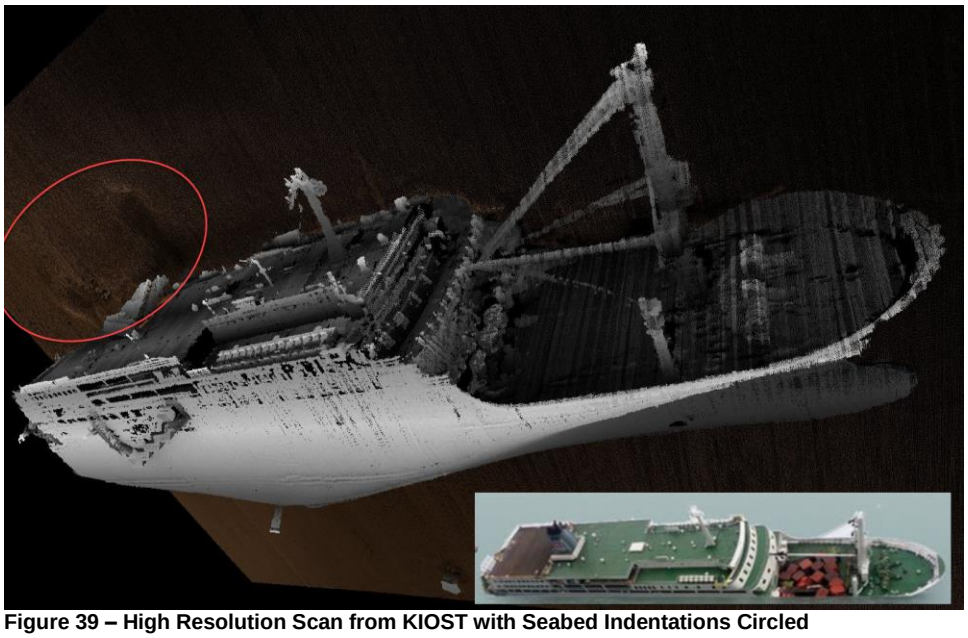

Figure 39 – High Resolution Scan from KIOST with Seabed Indentations Circled

Site Investigation Issues

The KIOST survey includes some 25 grab samples and 13 drop piston core samples. Of these only three grab samples were 250m from the wreck, and eight piston samples 500 to 600m from it.

Of the eight piston samples taken only two have penetrations consistent with even a medium dense gravelly seabed (130 and 260mm); four are in the range 400 to 960mm, and two at 1220 and 1610mm.

The authors have relied on these penetrations, rather than the content of the samples, since no direct access to the content was possible. Nevertheless, the description of the soil did agree with the author' s [eventual] interpretation, but no strength measurements from the samples were reported to us.

The KIOST sub-bottom profile data closest to the wreck was line 31 which ran parallel to it, and about 40m north; and line 11 which crossed just behind the bows of ship. These lines and KIOST's interpretation are illustrated in Figure 40 and Figure 41. A further line (12) crossed the stern, but no interpretation was given.

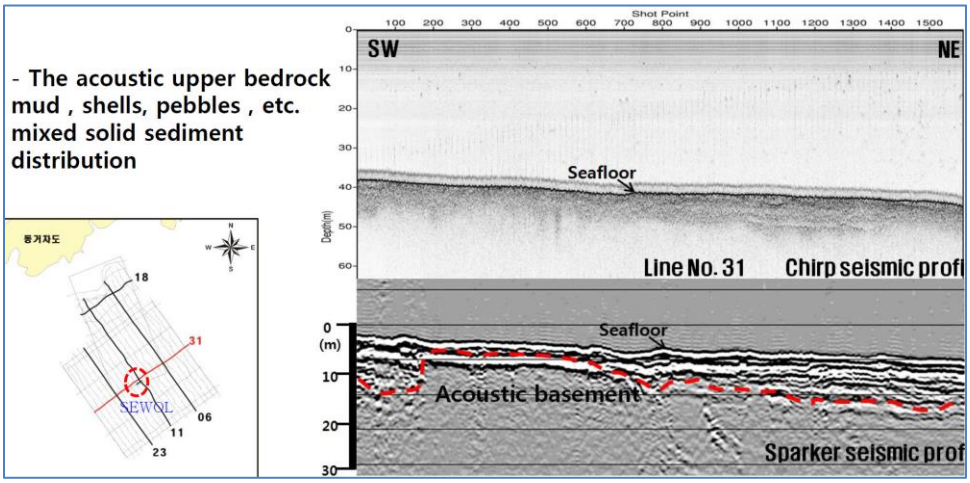

Figure 40 – KIOST Line 31

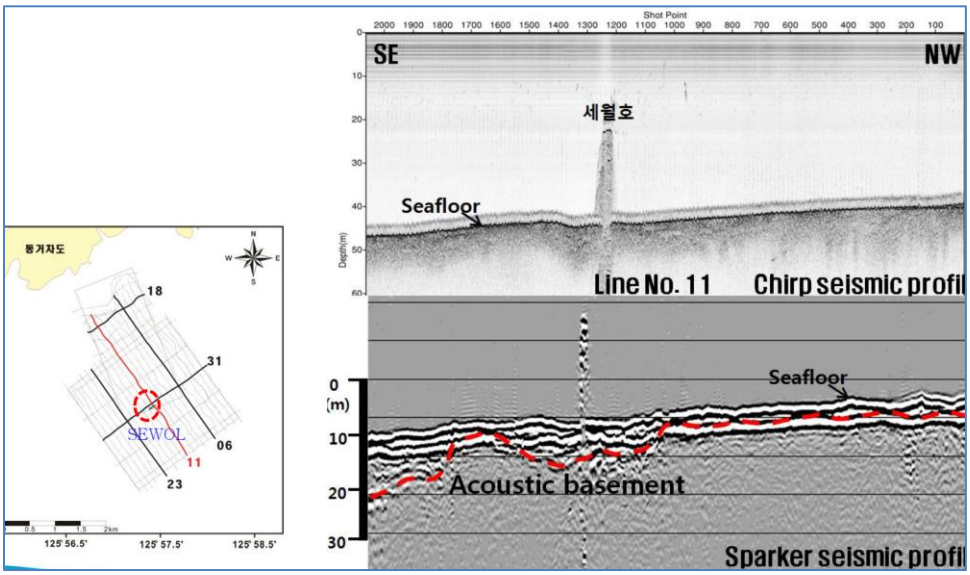

Figure 41 – KIOST Line 11

KIOST also supplied a notional interpretation of the sub-bottom profiler data in the form of a map of depth of surface deposits (Figure 42).

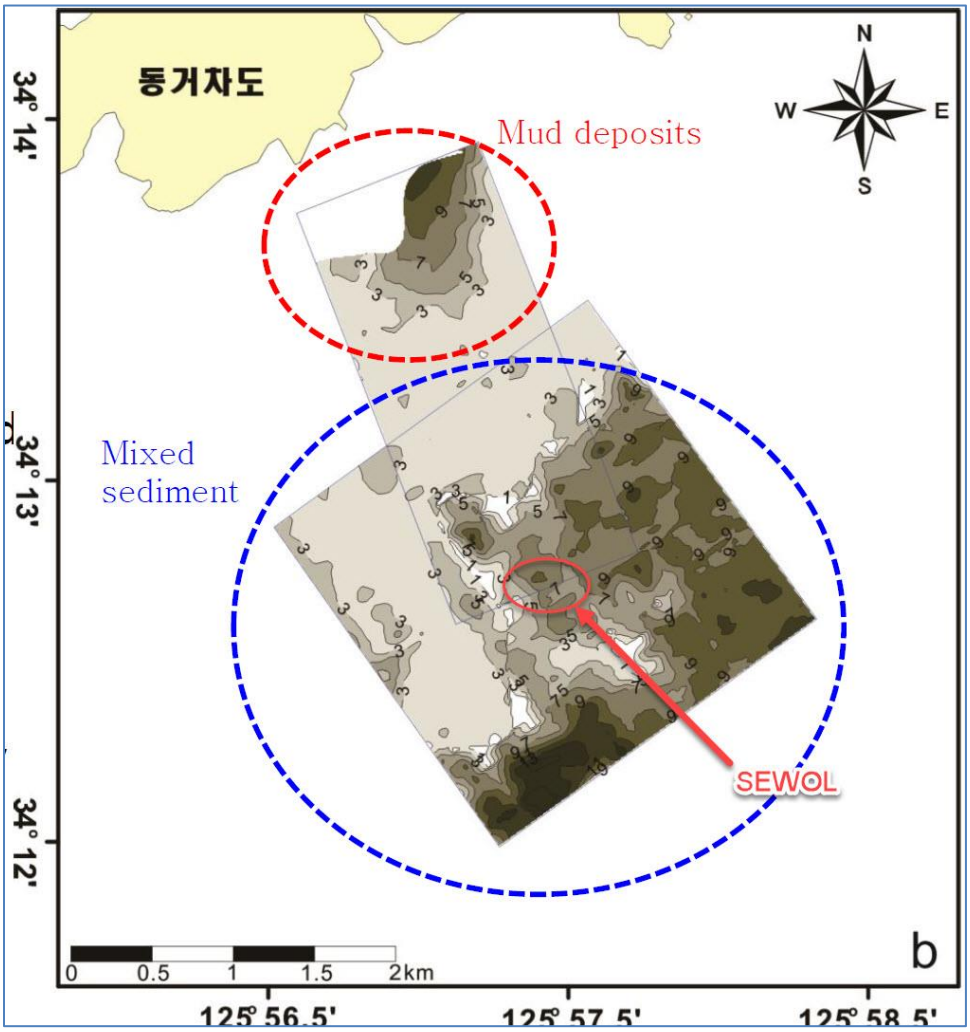

Figure 42 – KIOST Surface Deposit Map

The TIWT geotechnical investigation consisted of six boreholes drilled either side and 20m away at the aft, midships and bow of the wreck; and two boreholes 300m north and south of the bows, to investigate the site of two bow lateral restraint anchors planned for the bow lift. All boreholes were extended to 4m penetration and provided a nearly identical interpretation of conditions in each case, as above.

However, out of 32m of boreholes drilled, only a total of two metres of sample were recovered and tested. That is a recovery of 6.25%. The four boreholes most influential with respect to the bow lift were the two anchor boreholes, and the two at the stern, where the recovery drops to 2.5%. No samples were recovered from the two anchor boreholes. The test results are summarised in Table 3 below.

Project Name: Geotechnical Investigation for Savage Engineering of "Sewol" Wreck — Project No.: HYGC-2015-D1-19-1 — Date: 2015-09-16

Drilling hole No.	Soil sample No.	Sampling depth	Sampling state	Soil physical properties						Water ratio limit				Direct shear		Particle composition									Soil classification and engineering naming (Acoording <Engineering geology manual>)
				water content	specific gravity of soil	wet density	dry density	saturation	void ratio	liquid limit	plastic limit	plasticity index	liquidity index	cohesion	friction angle	pebble > 20.0	gravel 20.0 ~ 2.00	coarse sand 2.00 ~ 0.50	medium sand 0.50 ~ 0.25	fine sand 0.25 ~ 0.075	silt 0.075 ~ 0.05	silt (crude) 0.05 ~ 0.01	silt (fine) 0.01 ~ 0.005	clay < 0.005	
--	--	m	--	%	--	g/cm³		%	--	%	%	--	--	kPa	°	%	%	%	%	%	%	%	%	%	
SS-S-011~015	250101	1.50-1.70	undisturbed	20.0	2.70	1.92	1.50	94.5	0.800	25.6	16.0	9.6	0.42			14.2	29.4	10.8	4.1	10.2	5.9	14	3.1	8.3	Gravelly sand
SS-S-011~015	250103	3.00-3.20	undisturbed	18.0	2.70	1.96	1.66	77.7	0.626	23.0	15.3	7.7	0.35	16.8	28.6		10.6	10.3	4.6	14.8	23.4	21.4	4	10.9	Sandy cohensive soil
SS-S-016~020	250201	1.40-1.60	undisturbed	12.8		2.16	1.91									39	26.4	12.6	3.6	11.2	7.2				Little gravel
SS-S-016~020	250202	2.50-2.70	undisturbed	13.9		2.09	1.83									46.4	38	5.9	1.6	3.5	4.6				Little gravel
SS-S-016~020	250203	3.80-4.00	undisturbed	15.6	2.70	1.95	1.69	70.1	0.601	22.7	15.2	7.5	0.05			5.2	24.2	28.3	7.7	26.5	2.8	3.2	2.1		Gravelly cohensive soil
SS-S-021~025	250301	1.80-2.00	undisturbed	18.1	2.70	2.12	1.80	96.9	0.504	24.1	15.6	8.5	0.29			2.6	20	14.1	4.6	13.5	10	17.9	4.4	12.9	Silty sand
SS-S-021~025	250302	2.30-2.50	undisturbed	23.7	2.72	1.91	1.55	83.4	0.753	31.9	17.8	14.1	0.42	14.6	11.7		1.3	2	1	5	11.6	46.8	9.4	22.9	Cohensive soil
SS-S-021~025	250303	3.80-4.00	undisturbed	30.0	2.72	1.80	1.28	97.6	1.117	34.9	18.7	16.2	0.70	16.8	15.9	8.3	4.8	15.7	3.2	6.8	19.9	23.5	3	14.8	Sandy cohensive soil
SS-S-006~010	250501R	0.50-0.70	disturbed													82.3	14.7	1.4	0.4	0.6	0.6				Gravel
SS-S-001~005	250601	1.80-2.00	undisturbed	18.4	2.70	2.12	1.79	97.8	0.508	23.2	15.3	7.9	0.39				28.4	12	7.1	12.1	6.2	17.4	4.7	12.1	Gravelly sand
SS-S-001~005	250602	3.80-4.00	undisturbed	19.2	2.70	1.93	1.62	77.7	0.668	25.8	16.1	9.7	0.32				1.8	13.1	5.2	19.6	9	28.2	4.8	18.3	Cohensive soil

Table 3 – TIWT Reported Test Results

First Indication of Problems with Interpretation of Seabed Conditions

In an attempt to excavate a pit at the southernmost bow restraint gravity anchor location the conditions were found to be unlike those described by the site investigation. The design anchor depth was planned to be 5m below mudline. At 2m, following easy excavation of the surface layers, the clamshell dredge encountered bedrock (weathered granite) at a strength in the range weak to moderately weak. This was totally inconsistent with any of the interpretations given in the subject investigation reports.

The excavation process and form of the dug pit was at variance with the TIWT expectations. That is the upper layer stood vertically and was easily excavated. TIWT predicted "difficult to very difficult" dredgeability in the upper stratum. SSC did spend several days attempting to get below 2m, but the first part was easy.

The significant difference was the fact that the walls of the pit stood vertically to 2m depth implying a high fines and clay content, which is consistent with the logged description of the upper layer, and was consistently referred to as having between 55 and 60% "filler is clay". This of course is not borne out by the laboratory tests, but is an indicator of what the drillers observed, as illustrate by the borehole log in Figure 43.

All the samples tested from the investigation, with only a couple of exceptions, demonstrated a relative high fines content (silt and clay), which moves their behaviour toward that of clay. This review of the anchor pit excavation confirmed to the authors that the conditions were not as we had been led to believe, and tended to confirm our expectations.

Project name	Geotechnical Investigation for the Wreck of Sewol						
Project No.	HYGC-2015-D2-19-1			Drilling hole No.	SS-S-031~046		
Orifice height (m)	-45.00	Coordinate (m)	X = 3789428.01	Starting date	2015.8.21	Stable water depth (m)	Seawater
Orifice Diameter (mm)	150.00		Y = 772878.26	Completion Date	2015.8.22	Water level measurement date	

Layer No.	Geologic age and origin	Layer bottom elevation (m)	Layer bottom depthe (m)	Layer thickness (m)	columnar section 1:10	Geotechnical names and characteristics	Sampling	SPT blow count
①	Q_4^{pl}	-47.3	2.3	2.3		Gravelly soil: brown; dense, diameter is mainly 3~ 6cm, the largest particle size is 8cm, about 56%, filler is clay,Local containing cement.		
②	Q_3^{el}	-49.0	4.0	1.7		Residual soil: gray, plastic, mainly clayey soil with crushed granular, contain rock gravel.		

Survey institute	TianjinSurvey and Design Institute for transport Engineering

Figure 43 – Borehole Log at Location of Southeast Anchor Pit Excavation

Reinterpretation of Geotechnical Data

The salvage contractor at this stage, and even subsequently, resisted the temptation to obtain more and better seabed data, that is in spite of the author's recommendations to do so. The authors therefore resorted to reanalysis of the data to hand, and use of the "observational method". This took the following course:

1) reinterpretation of the limited laboratory test data as described by Table 3;
2) close examination of all seabed images from both the KIOST and TIWT surveys, including the influences of the wreck on the surface of the seabed;

3) as part of 2) a review of a 3D model/print derived from the KIOST survey;
4) observation of the efforts and outcome of salvage contractor's attempts to excavate and remove the ship's port side stabiliser fin; and
5) the excavation of the anchor pits and the subsequent anchor tests carried out within them.

The reinterpretation of the TIWT laboratory data concluded that the soil profile at the site consisted broadly of an upper layer of varying thickness of locally derived marine sands and gravels in a matrix of silty clay, with some layers of sand and gravel. The clay matrix exhibits lightly to moderately over-consolidated characteristics within a soft to firm strength range (cu 30 to 60 kPa). Back figuring the anchor test data gave clay shear strengths within this range.

The granular layers are thought to be loose to medium dense. These upper layers overlie the host material which created them. This material consists of weathered igneous rocks and associated residual soils created by the weathering process.

The thicknesses and strength of residual soils could not be determined from the data available. However, the weathered rocks defined in the anchor pits showed variable strength up to at least a weak rock classification.

As a part of the preparation for the bow lift the salvage contractor made efforts to remove the port side stabiliser fin. This involved the excavation, by air lift, of a pit adjacent to it. This excavation stood to a depth of two metres with near vertical sides. When eventually the fin (around 6m in length) was located, it was found to be undamaged and in its original position on the hull. This large impromptu penetration test shows that the upper layer of the seabed behaved more like a firm clay, than a dense gravel as the salvage contractor had been led to believe.

Figure 38 above, taken from the KIOST survey report, shows three ringed areas of the seabed which have been altered by the landing of ship.

KIOST note in their report that the wreck has rotated 10° clockwise and moved about 5m southeast from its original position in April 2014. This movement perhaps explains the berm of soil pushed-up/dozed forward by the keel. This berm was found to be at most 5m wide and 1.3m higher than the surrounding seabed.

This rotational movement has also disturbed the soil adjacent to the stern (Figure 44, taken from the KIOST 3D model of the survey data). This shows that the seabed has been altered by the lateral movement of the upper surface of the port side of the stern deck, and appears as a cohesive mass. That is the converse of the keel side berm already referred to.

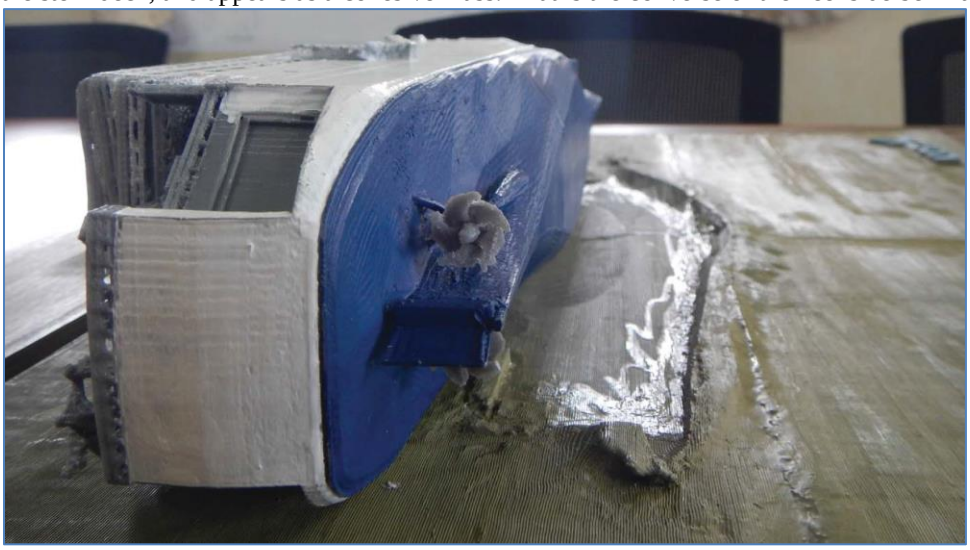

Figure 44 – Sewol 3D Printed Model by KIOST with Sewol Moved Sideways to Show Seabed

The two ringed areas of seabed on the upper side of the wreck are the scars left by the initial impact of the vessel. That is:

- first impact on the seabed being caused by the port-side stern end of the superstructure (resulting in the collapse of the port side corner of the upper deck. (See Figure 45);
- the second impact and scar relates to the funnel being crushed just before rollover takes place (See Figure 39 above)
- The "funnel scar" lies directly beside where the damaged funnel is now.

Figure 45 – Sewol 3D Printed Model by KIOST Showing Topside and Adjacent Seabed

It is speculated that the first impact of the upper deck, the "superstructure scar", is about 20m away from the damage. This suggests that the vessel, under failing buoyancy conditions, drifted ten to twenty metres north east after the first impact. In fact this scar shows two depressions in a line going southeast, suggesting that the damage was caused by two impacts. The vessel was lying in the water, mostly submerged, at an angle of 29° upon first impact.

What was surprising about the examination of the TIWT data concerning the above seabed scars is their relatively shallow nature. Although the data was limited, it was sufficient to show that, at the site of the upper deck impact, there is an indentation in the seabed of less than a metre. This was the impact which crushed the entire corner of the accommodation below it, and compressed it by 2.5m.

Similarly, the funnel scar is relatively shallow, less than a metre, but with a heaved area at the northwest end about 0.7m high. The depressions caused by these impacts were unexpectedly small but at the time were not seen to be important. That changed later.

All the samples tested from the investigation with only a couple of exceptions demonstrated a relative high fines content (silt and clay), which moves their behaviour toward that of clay.

The review of the anchor pit excavation confirmed to STA that the conditions were not as we had been led to believe, and tended to confirm our expectations.

The Second Cause for Concern Arising Out of Poor Site Investigation Practice

As already noted the bow lift (both attempts) gave rise to the heeling problem the authors had warned of from the outset.

Since the surface soils were softer than expected by the salvage contractor, not only did the stern penetrate significantly during the bow lift, but of course the superstructure during heeling, pushed further into the seabed.

Also after the forward lifting beams had been placed and the hook released, the wreck did not lay back down fully at the bow, and it is likely that some of the beams pushed into the seabed. This made the gap available to insert the remaining beams at the stern much less than desirable, making it necessary to drag soil from below the hull.

It soon became apparent that the heeled wreck at its northwest side was now very close to rock-head which had not been identified by the site investigation. This of course made it almost impossible to insert some of the lifting beams. The proximity of the rock-head could also be the explanation for the shallow depressions caused by the initial impacts.

Geotechnical Lessons Learned

Whereas the authors were not given the chance to fully analyse the shortcomings arising from the site survey and investigation, a properly engineered and supervised investigation would have avoided many of the problems faced.

It seems likely that sub-bottom profiler data had been wrongly interpreted, and no effort had been made to prove that the data was consistent with borehole records. This used to be known as "ground truthing".

Had more attention been paid to the avoidance of heeling, then it would probably have been possible to stay away from the unseen geo-hazards that lay below the seabed.

Summary

The Sewol Salvage project began in 2015 and was planned to be complete, with the Sewol on land in one piece, before the end of 2016. This did not happen.

The main causes of delay were a failure to address the importance of heeling control during bow lifting operations and a failure to undertake a more thorough geotechnical site investigation.

Secondary causes included poor attention to weather forecasts and a lack of belief that relatively large dynamic forces could be caused by quite small waves if wave periods were relatively long.

A poor detail where slings passed around a deck edge resulted in a tearing failure.

Time domain fully-coupled OrcaFlex hydrodynamic dynamic analysis was used to define limiting environmental conditions for safe lifting. Limiting conditions were sling maximum tensions and Sewol buckling stresses.

References

[1] A. Guha, "Development and application of a potential flow computer program: Determining first and second order wave forces at zero and forward speed in deep and intermediate water depth," Texas A&M University, College Station, TX, 2016.